Journal of
Medicinal Chemistry

Article

Peptide-#-lactam inhibitors of dengue and West Nile virus NS2B-NS3 protease display two distinct binding modes

Tonko Drazic, Sara Kopf, James F. Corridan, Mila M. Leuthold, Branimir Bertosa, and Christian D. Klein

J. Med. Chem., **Just Accepted Manuscript** • DOI: 10.1021/acs.jmedchem.9b00759 • Publication Date (Web): 05 Dec 2019

Just Accepted

is published by the American Chemical Society. 1155 Sixteenth Street N.W., Washington, DC 20036

Peptide-β-lactam inhibitors of dengue and West Nile virus NS2B-NS3 protease display two distinct binding modes

Tonko Dražić,[*,†] Sara Kopf,[†,§] James Corridan,[†,‡] Mila M. Leuthold,[†] Branimir Bertoša,[#] and Christian D. Klein[†]

[†]Medicinal Chemistry, Institute of Pharmacy and Molecular Biotechnology IPMB, Heidelberg University, Im Neuenheimer Feld 364, 69120 Heidelberg, Germany

[#] Department of Chemistry, Faculty of Science, University of Zagreb, Horvatovac 102a, 10 000 Zagreb, Croatia

ABSTRACT The β-lactam ring represents a valuable moiety that can induce covalent binding of an inhibitor to its target. In this study, we explored di- and tripeptides with β-lactam electrophilic warheads as inhibitors of dengue and West Nile virus NS2B-NS3 protease. Tripeptides with a (3*S*)-β-lactam moiety displayed highest activity, with IC_{50} and EC_{50} values in the lower micromolar range in biochemical and cellular assays. The activity against dengue protease was in general higher than against West Nile virus protease. The compounds were inactive against the off-targets thrombin and trypsin. LC-MS experiments revealed that tripeptide-β-lactam inhibitors bind to the protease in two distinct binding modes. Only one binding mode leads to a covalent, but reversible, interaction of the β-lactam ring with the catalytic serine, followed by release of the inhibitor with opened β-lactam ring. The other binding mode leads to the cleavage of the peptide backbone. This observation provides the first experimental evidence that benzyloxyphenylglycine in flaviviral protease inhibitors is positioned in the prime site of the enzyme.

Introduction

Covalent inhibitors have long been stigmatized in drug discovery as toxic and harmful entities. However, in recent years the interest for this class of compounds has significantly increased, which has resulted in several covalent drug candidates and approved covalent drugs on the market today.[1] Some of the examples include kinase inhibitors[2,3] and proteasome inhibitors[4] as anti-cancer agents, as well as drugs against hepatitis C virus, which target the viral protease.[5] Acrylamides, α-ketoamides, epoxyketones and boronic acids are some of the groups that serve as electrophilic warheads and induce covalent binding between the inhibitor and the target protein.[6]

Compounds containing electrophilic warheads have also been investigated as inhibitors of flaviviral NS2B-NS3 proteases. Flaviviruses, including dengue (DENV) and West Nile virus (WNV), represent a serious threat to human health. For DENV alone there are an estimated 390 million infections per year.[7] In addition, predictions suggest that cases of dengue and other flaviviral related diseases will increase in future.[8,9] NS2B-NS3 protease represents a valuable pharmacological target for the development of antiflaviviral drugs, as it cleaves flaviviral polyprotein and therefore, its activity is necessary for viral replication.[10] In addition, NS2B-NS3 is a serine protease, which makes it a favorable target for covalent inhibitors. Until today a number of peptide-based inhibitors of dengue virus protease have been developed, some of them containing electrophilic warheads (Figure 1).[11] Yin et al. were the first to employ the strategy of incorporating C-terminal warheads into substrate-mimicking peptide inhibitors (Figure 1B).[12,13] In their research, several electrophiles were evaluated, but the main focus was given to aldehyde warheads. The incorporation of C-terminal aldehyde increased the affinity of the peptide inhibitor more than 20 fold, with a K_i value reaching 5.8 μM. Interestingly, the boronic acid analog had an even more profound effect (K_i = 43 nM), yet inhibitors containing this moiety were not investigated in more detail in this study. Subsequent characterization of peptide-boronic acids demonstrated that dipeptides containing unnatural basic amino acids and C-terminal boronic acid moieties (Figure 1B) can reach low nanomolar IC_{50} values in a biochemical assay and that the activity highly depends on the presence of this functional group. However, this type of compounds also showed a pronounced off-target effect by inhibiting trypsin in the same range or higher than flaviviral proteases. Additionally, the activity in cell-based viral replication assay was significantly lower than in the biochemical assay.[14]

Herein we report peptide inhibitors of NS2B-NS3 protease bearing a C-terminal β-lactam moiety. Having in mind the positive impact of electrophilic warheads on the activity, as well as their obvious drawbacks, we reasoned that β-lactam is a promising moiety to induce covalent binding to the NS2B-NS3 protease. With a "soft" reactivity that can be modulated by changing the character of substituents, the β-lactam moiety may mitigate liabilities encountered in the development of antiflaviviral covalent drugs (*e.g.* low drug-likeness of the warhead or off-target effects). The β-lactam group as an electrophilic moiety is, despite importance in antibacterial agents, surprisingly underexploited in other areas of medicinal chemistry. To the best of our knowledge, in the last ten years the β-lactam moiety has been integrated only in the development of *N*-acylethanolamine acid amidase (NAAA) inhibitors, an enzyme which is a potential target for anti-inflammatory drugs.[15–17] Before

that, only several β-lactam inhibitors of other serine proteases, such as thrombin and elastase, have been described.[18,19]

It is often considered that β-lactam reactivity stems from steric strain caused by the fused second ring (*e.g.* penam and cephem antibiotics) or by strong electron withdrawing substituents at N-1 position (*e.g.* monobactam antibiotics). However, even in the absence of these structural properties, β-lactam moieties in NAAA inhibitors (*i.e.* N-1 unsubstituted β-lactam) and elastase inhibitors (*i.e.* β-lactam with N-1 aromatic substituent) still show time-dependent inhibition that is derived from covalent binding to their targets.[20,21] Therefore, we decided to use β-lactams with an aromatic substituent at N-1 position, as we expected such β-lactams to have mild reactivity due to the moderately electron withdrawing N-1 group. We hoped that this type of β-lactams would enable covalent binding to the target, but at the same time alleviate off-target binding. β-Lactams were combined with di- and tripeptides that previously showed affinity for NS2B-NS3 protease, to serve as a recognition element of the inhibitor. We explored the effect of different peptides on the activity, as well as the influence of the stereochemistry on the β-lactam C-3 stereocenter and electronic effect of N-1 aryl substituent. Together with the evaluation of the activity in biochemical and cellular assays, the inhibition mechanism of the most active compounds was investigated.

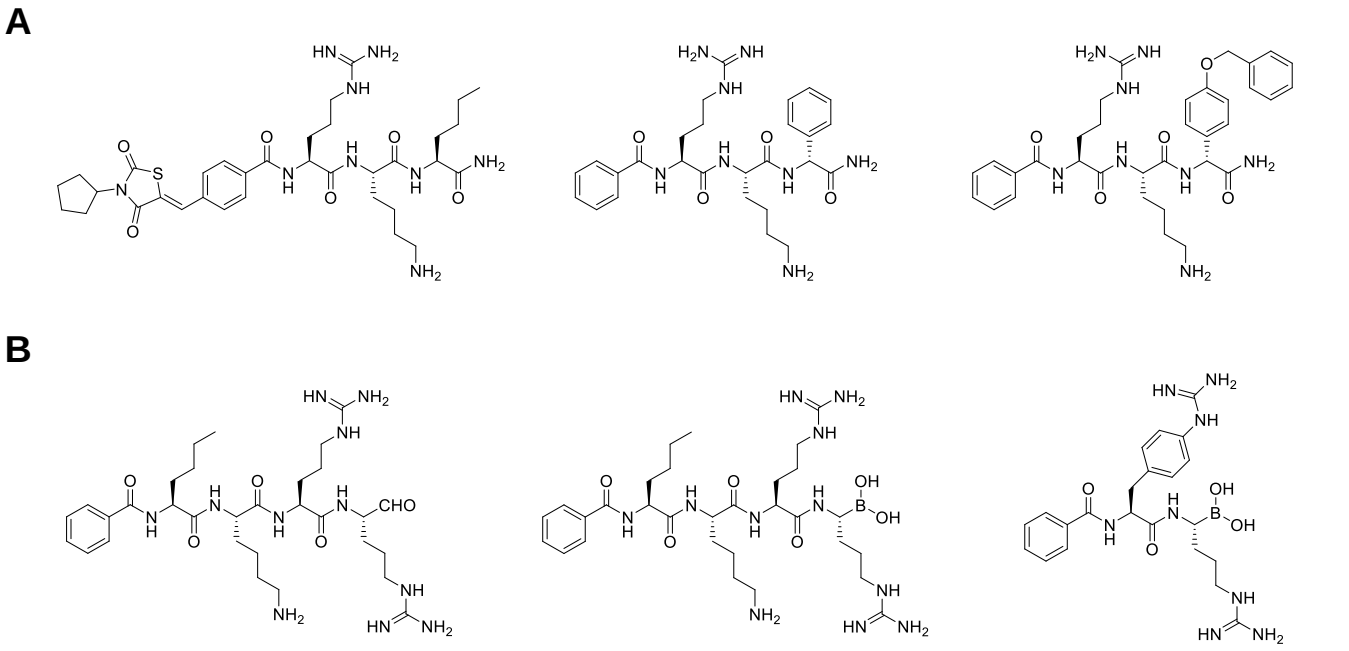

Figure 1. Examples of previously developed peptide inhibitors of flaviviral NS2B-NS3 protease. **A)** Inhibitors containing heterocyclic *N*-terminal caps and unnatural amino acids. **B)** Inhibitors containing C-terminal electrophilic warheads. The details about the compounds can be found further in the text, as well as in references 11 (in ref. 56), 29 and 23 for compounds in figure A and for compounds in figure B in references 12, 12 and 14. The references are given in the consecutive order.

Results and discussion

Chemistry

Synthesis of β-lactams (3*R*)- and (3*S*)-3a–e. β-Lactams **3a**–**e** were obtained in a three-step reaction sequence starting from Cbz-protected serine.[15,22] This method enables the preparation of enantiopure (3*R*)- and (3*S*)-β-lactams using the predetermined chirality of (*S*)- or (*R*)-serine, respectively. It also gives β-lactams with N-1 aryl substituent and a free amino group at the C-3 position, which facilitates coupling to the peptides (Scheme 1). The first step is the coupling of an aryl amine to the serine C-terminus, which was obtained using COMU as a coupling reagent and TMP as a base. The main step is the cyclization of amides (*S*)- and (*R*)-**1a**–**e** into β-lactams (3*R*)- and (3*S*)-**2a**–**e**. The reaction proceeded with the addition of 1,1'-sulfonyldiimidazole and sodium hydride. 1,1'-Sulfonyldiimidazole was used to facilitate the ring closure by activating the hydroxyl group through the formation of imidazole-1-sulfonate leaving group. β-Lactams (3*R*)- and (3*S*)-**2a**–**e** were obtained in 34–76% yield. In the last step Cbz-protection was cleaved using hydrogen and palladium on charcoal, providing the enantiomerically pure 3-amino-β-lactams (3*R*)- and (3*S*)-**3a**–**e**.

Synthesis of dipeptide-β-lactam inhibitors. *N*-Benzoyl-capped dipeptides were obtained by SPPS on CTC resin using the Fmoc-protocol with COMU and TMP.[23] The protected dipeptides were coupled to β-lactams (3*R*)- and (3*S*)-**3a** using the mixed-anhydride method with IBCF and NMM as a base (Scheme 2).[24] Final inhibitors (3*R*)- and (3*S*)-**4**–**8** were obtained in low to moderate yields after lysine/arginine deprotection (Table S1, Supporting information). The coupling efficiency depended on the amino acid at P1 position, with lysine showing the highest reactivity while arginine and norleucine gave significantly lower yields.

Synthesis of tripeptide-β-lactam inhibitors. Initially, we attempted to couple β-lactams **3a**–**e** directly to the Bz-Arg(Pbf)-

Lys(Boc)-(4-benzyloxy)-D-Phg-OH tripeptide. We tried several different coupling reagents (*i.e.* COMU, HATU, IBCF), which were not successful. Therefore, we explored an alternative two-step coupling route, in which the β-lactam is first coupled to Fmoc-(4-benzyloxy)-D-Phg-OH **9**, followed by coupling to Bz-Arg(Pbf)-Lys(Boc)-OH dipeptide (Scheme 3). This strategy was successful and afforded the final tripeptide-β-lactam inhibitors in sufficient quantities. For both coupling steps, COMU and TMP were used applying a previously described protocol.[25] (4-Benzyloxy)-D-Phg-β-lactam derivatives (3*R*)- and (3*S*)-**10a**–**e** were obtained in 23–50% yield after the coupling and Fmoc deprotection steps, whereas the final (3*R*)- and (3*S*)-**11a**–**e** were isolated in 11–57% yield after two steps. We observed epimerization of the final product at the (4-benzyloxy)-D-Phg α-C position. The epimerization is probably the consequence of the basic work-up after Boc/Pbf deprotection, as it is known that phenylglycine and its derivatives are susceptible to racemization, especially under basic conditions.[26] The ratio of (4-benzyloxy)-D-Phg epimers was evaluated independently by HPLC and ^{1}H NMR (Figure S1, Supporting information). The determined values correlated well between the methods. In most products, the epimerization was between 10% and 20%, except in compounds (3*R*)-**11d** and **e** where the ratio of (*R*)- and (*S*)-(4-benzyloxy)-Phg epimers was ~ 65 : 35 (Table S2, Supporting information). The epimerization on the β-lactam ring was not observed in any of the products.

Scheme 1. Synthesis of β-lactams (3*R*)- and (3*S*)-3a–e.

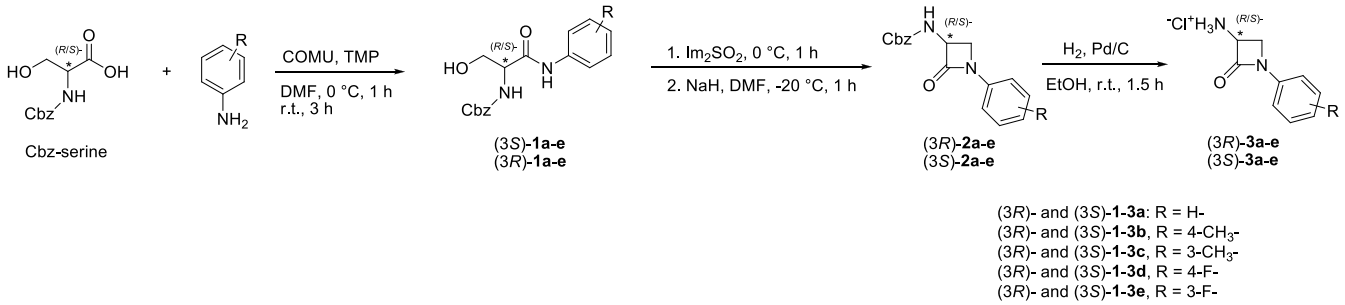

Scheme 2. Synthesis of dipeptide β-lactam inhibitors (3*R*)- and (3*S*)-4–8.

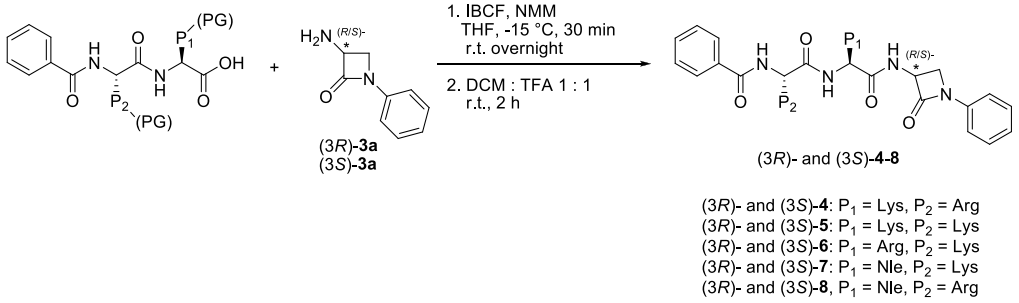

Scheme 3. Synthesis of tripeptide inhibitors 11a–e.

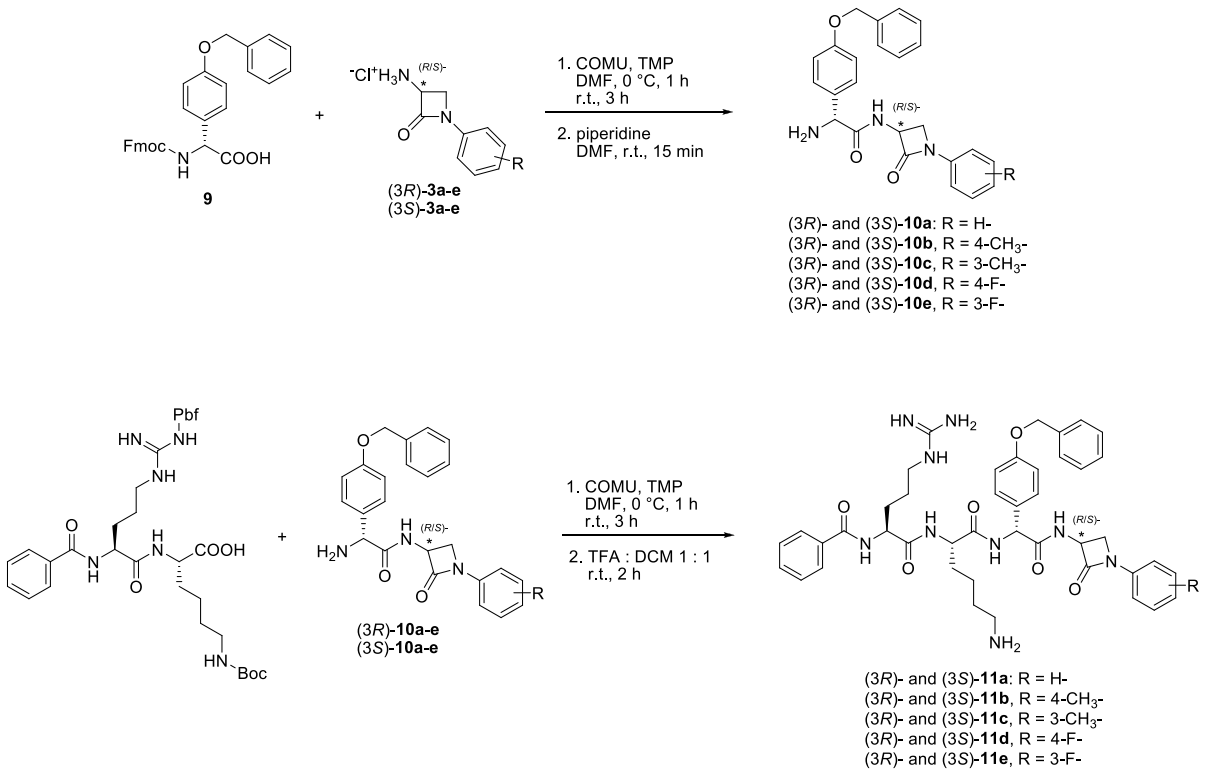

Biology

Activity of peptide-β-lactam inhibitors in biochemical assays. The activity of dipeptide-β-lactam derivatives (3*R*)- and (3*S*)-**4**–**8** was initially screened at 50 μM concentration against DENV and WNV NS2B-NS3 protease. Among the tested sequences, inhibitors with the amino acid sequence Bz-Arg-Lys showed the highest activity (Table 1). Compound (3*R*)-**4** with (3*R*)-β-lactam had 72% inhibition of DENV protease, with IC_{50} = 17.7 μM, whereas the (3*S*)-β-lactam analog showed 57% inhibition (IC_{50} value not measured). Both values represent an increase in the inhibition compared to the previously investigated parent dipeptide without β-lactam moiety, which gave 41% inhibition at 50 μM concentration and IC_{50} = 58.5 μM (IC_{50} value calculated from K_i given in the reference using Cheng-Prusoff equation, K_m = 105 μM).[27] Replacement of the P_2 arginine with lysine in compounds (3*R*)-**5** and (3*S*)-**5** decreased the activity of both compounds against DENV protease, as well as of (3*S*)-**5** against WNV protease. On the other hand, the same replacement slightly increased the inhibition of (3*R*)-**5** isomer against WNV protease. The inversion of the peptide sequence Bz-Arg-Lys-β-lactam to Bz-Lys-Arg-β-lactam, as well as the incorporation of non-basic norleucine at P_1 position led to complete loss of activity in both enzymes. The loss of activity in WNV protease upon the sequence inversion is in contrast to previous reports where the preference for P_2 lysine in WNV protease or arginine in case of DENV protease was observed.[27,28]

Previously, tremendous improvements in the activity of peptide NS2B-NS3 protease inhibitors were achieved with the incorporation of the unnatural amino acids phenylglycine and benzyloxyphenylglycine at P_1 position (Figure 1A).[23,29] For example, tripeptide Bz-Arg-Lys-(4-benzyloxy)-D-Phg-NH_2 (**MB-53**, cpnd. 27 in the reference)[23] had IC_{50} = 0.37 μM against DENV protease, which is a profound increase relative to dipeptide Bz-Arg-Lys-NH_2[27] with IC_{50} = 58.5 μM (see above). In order to investigate if a similar effect would be achieved in peptide-β-lactam inhibitors, we synthesized compounds with sequence Bz-Arg-Lys-(4-benzyloxy)-D-Phg-β-lactam, where β-lactam had either (3*R*)- or (3*S*)-configuration ((3*R*)- and (3*S*)-**11a**). The incorporation of (4-benzyloxy)-D-Phg had a different effect on the activity depending on the β-lactam configuration (Table 2). In the case of Bz-Arg-Lys-(4-benzyloxy)-D-Phg-(3*S*)-β-lactam derivatives, the activity significantly improved, although not reaching the activity of **MB-53**. Inhibitor (3*S*)-**11a** had 96% inhibition at 50 μM concentration with IC_{50} = 2.6 μM, whereas dipeptide without benzyloxyphenylglycine (3*S*)-**4** gave 57% inhibition at 50 μM concentration (IC_{50} value not measured). On the other hand, the integration of (4-benzyloxy)-D-Phg in inhibitors containing (3*R*)-β-lactam had no significant effect, as tripeptide (3*R*)-**11a** and its dipeptide counterpart (3*R*)-**4** had similar activities (69% and 72% inhibition at 50 μM concentration, respectively).

We further investigated the effect of the β-lactam N-1 substituent on the inhibition. It can be assumed that the character of an aryl substituent plays a role in the reactivity of the β-lactam. We expected that an electron withdrawing substituent would increase the reactivity of the β-lactam carbonyl group and, consequently, improve the activity. However, substituents at N-1 had no effect on the inhibition, as all inhibitors in the (3*S*)-**11** series had very similar IC_{50} values (1.9–2.8 μM), whereas the (3*R*)-series showed no correlation between the substituent nature and the inhibition. The activity against WNV was generally lower compared to DENV in all tripeptide-β-lactam inhibitors (Table 2).

Table 1. Activity of dipeptides 4–8 in biochemical assays.

Compound	DENV (%)	WNV (%)	Compound	DENV (%)	WNV (%)
(3*R*)-**4** 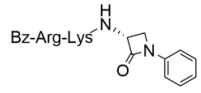	71.6% IC_{50}= 17.7 μM	27.8%	(3*S*)-**4** 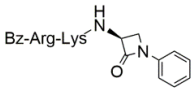	57.1%	81.4% IC_{50}= 22.5 μM
(3*R*)-**5** 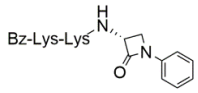	39.7%	51.7%	(3*S*)-**5** 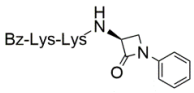	n.i.	n.i.
(3*R*)-**6** 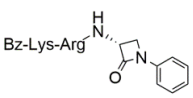	n.i.	n.i.	(3*S*)-**6** 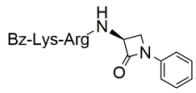	n.i.	n.i.
(3*R*)-**7** 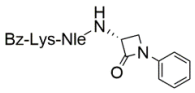	n.i.	24.4%	(3*S*)-**7** 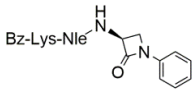	n.i.	n.i.
(3*R*)-**8** 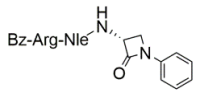	n.i.	n.i.	(3*S*)-**8** 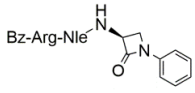	n.i.	n.i.

DENV: enzyme 100 nM; substrate 50 μM; percent values at inhibitor 50 μM; IC_{50} values determined if inhibition > 70% at 50 μM.

WNV: enzyme 150 nM; substrate 50 μM; percent values at inhibitor 50 μM; IC_{50} values determined if inhibition > 70% at 50 μM.

n.i. = inhibition < 20%

Table 2. Activity of tripeptides 11a–e in biochemical assays.

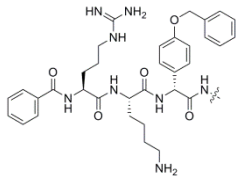

Compound	DENV	WNV	Compound	DENV	WNV
(3*R*)-**11a** 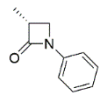	68.8%	46.9%	(3*S*)-**11a** 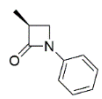	96.0% IC_{50} = 2.3 μM	60.1%
(3*R*)-**11b** 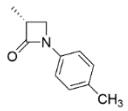	73.5% IC_{50} = 15.9 μM	52.9%	(3*S*)-**11b** 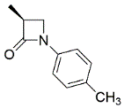	95.9% IC_{50} = 2.7 μM	60.3
(3*R*)-**11c** 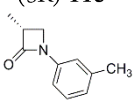	77.7% IC_{50} = 16.4 μM	45.1%	(3*S*)-**11c** 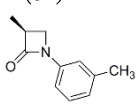	96.5% IC_{50} = 2.8 μM	46.8%
(3*R*)-**11d** 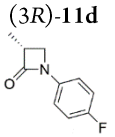	65.5%	43.4%	(3*S*)-**11d** 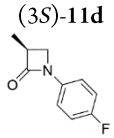	96.3% IC_{50} = 2.5 μM	60.9%

(3*R*)-**11e** 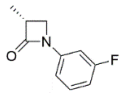	80.8% IC_{50} = 12.4 μM	61.6%	(3*S*)-**11e** 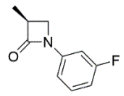	96.8% IC_{50} = 1.9 μM	64.1%

DENV: enzyme 100 nM; substrate 50 μM; percent values at inhibitor 50 μM; IC_{50} values determined if inhibition > 70% at 50 μM.

WNV: enzyme 150 nM; substrate 50 μM; percent values at inhibitor 50 μM.

Off-target effects. The activities of compounds (3*R*)- and (3*S*)-**4**–**8**, as well as (3*R*)- and (3*S*)-**11a–e** against thrombin and trypsin as off-target serine proteases with similar substrate recognition motifs was evaluated. Tripeptide-β-lactam inhibitors (3*R*)- and (3*S*)-**11a**–**e** showed high selectivity for flaviviral proteases, with inhibition against both thrombin and trypsin < 20% at 50 μM inhibitor concentration. Similar selectivity was observed in dipeptide derivatives, with only compounds (3*R*)-**5**, (3*R*)-**7** and (3*S*)-**8** slightly exceeding 20% inhibition against trypsin (Table S3, Supporting information).

Binding mode of tripeptide-β-lactam derivatives. The binding mode of compound (3*S*)-**11a** was investigated using a tryptophan quenching assay.[30] This assay is based on the intrinsic fluorescence of tryptophan near the active site of DENV protease. The assay also includes a competitor molecule (quencher) that binds competitively to the protease causing a decrease in the fluorescence signal upon binding. When the inhibitor is added together with the quencher, the increase in fluorescence (decrease of quenching) compared to the quencher control indicates competitive binding of the inhibitor. As a quencher, we used compound **MB-211** (Figure S5, Supporting information), which was previously characterized as a competitive inhibitor of DENV protease (IC_{50} = 0.176 μM) and has an absorption band in the tryptophan emission region.[23] Inhibitor (3*S*)-**11a** in concentrations 20 μM and 60 μM was added to the protease together with the quencher **MB-211** (concentration range 0–20 μM). The addition of the inhibitor in both concentrations caused a decrease in quenching compared to the **MB-211** control (Figure 2). Furthermore, the decrease was concentration dependent. This clearly demonstrates that inhibitor (3*S*)-**11a** binds competitively to the active site of DENV protease.

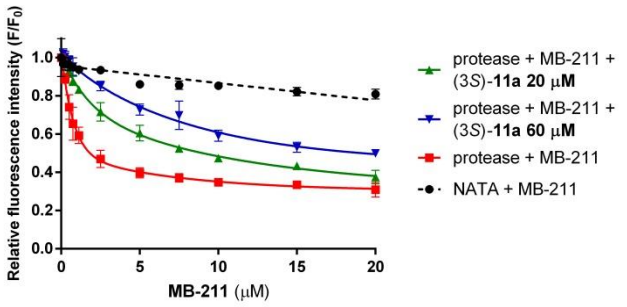

Figure 2. Change in DENV protease intrinsic fluorescence by the addition of **MB-211** in combination with (3*S*)-**11a** 20 μM (green line) or (3*S*)-**11a** 60 μM (blue line) in relation to **MB-211** control (red line). The interference by inner filter effect (IFE) was evaluated using *N*-acetyltryptophanamide (NATA) instead of DENV protease (dashed line).

The tryptophan quenching assay was also used to study the reversibility of (3*S*)-**11a** binding to the protease. The theoretical background of the experiment lies in the fact that irreversible binding of the inhibitor, when preincubated with the protease, would prevent binding of the quencher and consequently, quenching would not be observed upon the addition of the quencher. Therefore, inhibitor (3*S*)-**11a** at 60 μM concentration was preincubated with DENV protease for 16 hours before the addition of quencher **MB-211**. The quenching after concurrent addition of (3*S*)-**11a** and **MB-211** served as a control. The preincubation of the protease with (3*S*)-**11a** had no effect on quenching, indicating that (3*S*)-**11a** binds reversibly to the protease (Figure 3).

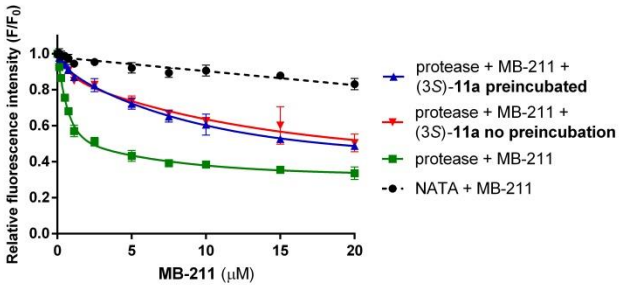

Figure 3. The change in DENV protease intrinsic fluorescence by the addition of **MB-211** after 16 h incubation with (3*S*)-**11a** 60 μM (blue line), **MB-211** with (3*S*)-**11a** 60 μM without preincubation (red line), **MB-211** without (3*S*)-**11a** (green line) and **MB-211** in combination with *N*-acetyltryptophanamide (NATA) instead of DENV protease as IFE (dashed line).

Reversible binding of (3*S*)-**11a** was additionally evaluated with the dilution experiment, in which the target enzyme is preincubated with an inhibitor at high concentration, after which the inhibitor is diluted to approximately one half of the IC_{50} value and the activity of the enzyme is measured over time.[31] Inhibitor (3*S*)-**11a** at the concentration 60 μM (~ 20 × IC_{50}) was preincubated with the DENV protease for either 3 or 6 hours, then diluted to 1.7 μM (~ half IC_{50}) and the activity of the protease was measured for 2 hours in 30 minute intervals. Four controls were included in the experiment: DMSO control to monitor the full activity of the protease, high concentration inhibitor control (60 μM) to achieve complete inhibition of the protease, one half IC_{50} control (1.7 μM) without preincubation and one half IC_{50} control (1.7 μM) with preincubation (3 h or 6 h) as a reference inhibition of the sample after dilution. Compound (3*S*)-**11a** did not show increased inhibition after dilution in comparison to the one half IC_{50} controls, therefore confirming reversible nature of binding (Figure 4). Furthermore, the inhibition of the diluted sample remained constant throughout the 2 hour measurement period. Very similar results were obtained

for both 3 hour and 6 hour preincubation period, which further indicates that the preincubation of the inhibitor with the protease does not result in a time-dependent, irreversible inhibition.

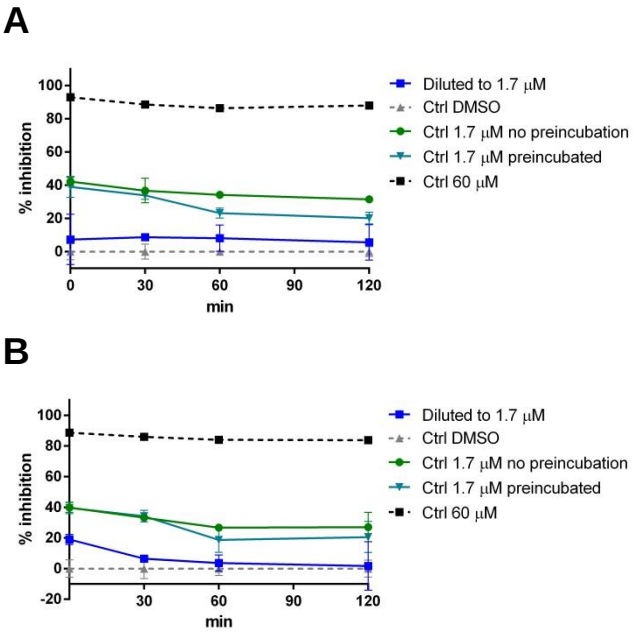

Figure 4. Dilution experiment for compound (3*S*)-**11a**. The sample diluted from 60 μM to 1.7 μM after preincubation is presented as blue line, relative to full activity (DMSO) control (grey dashed line), full inhibition (60 μM) control (black dashed line), one half IC_{50} (1.7 μM) without preincubation control (green line) and one half IC_{50} (1.7 μM) with preincubation control (cyan line). **A)** The inhibition after 3 h preincubation of (3*S*)-**11a** with DENV protease. **B)** The inhibition after 6 h preincubation under the same conditions.

In order to investigate the role of the catalytic serine on the binding of tripeptide-β-lactam inhibitors, DENV protease with S135A mutation was expressed. The binding affinity of the inhibitor (3*S*)-**11a** towards the S135A mutant was evaluated using tryptophan quenching assay. First, the effect of the mutation on the binding of the quencher **MB-211** was determined (Figure S6, Supporting information). **MB-211** binds to the catalytic site of the mutant with reduced affinity in comparison to the active protease. On the other hand, the binding affinity of (3*S*)-**11a** towards the mutant protease was almost completely lost, as the quenching upon the addition of (3*S*)-**11a** in the concentrations 20 μM and 60 μM in combination with **MB-211** was minimally changed compared to **MB-211** control (Figure S7, Supporting information).

Finally, we performed LC-MS experiments in order to identify potential covalent binding of the inhibitor to the protease. First, we focused on detecting MS adducts of the inhibitor with DENV protease. However, after several attempts applying different methods, we were not able to observe any adduct formation. We then turned our attention to identifying a change in the inhibitor mass which would be a consequence of covalent binding. We incubated compound (3*S*)-**11a** for 11 h with either active DENV protease, inactive S135A mutant or buffer without the protease, and monitored the modification of the inhibitor through time. The change in the inhibitor mass during incubation revealed a complex inhibition mechanism. During the course of the experiment, the β-lactam form of inhibitor was depleted and a mass that corresponds to an analog with opened β-lactam ring **12** (m/z $[M - H]^-$ = 806.3984) appeared in the spectrum (Figure 5 and Figure S8, Supporting information). However, the main effect was the appearance of peaks at m/z $[M - H]^-$ = 405 and m/z $[M - H]^-$ = 400. These two masses correspond to Bz-Arg-Lys-OH **13** (m/z $[M - H]^-$ = 405.2249) and benzyloxyphenylglycine-β-lactam **14** (m/z $[M - H]^-$ = 400.1656). The formation of **13** and **14** is a consequence of the cleavage of the amide bond between lysine and benzyloxyphenylglycine. Both changes are apparent only during incubation with the active protease (Figure 5A and C). This indicates that the inhibitor (3*S*)-**11a** can adopt two conformations in the active site, one in which lysine carbonyl group lies close to the catalytic serine and the other where β-lactam ring is in close proximity to the serine, enabling the reaction of the corresponding carbonyl group with the serine. The binding of the inhibitor in two distinct ways might be possible due to conformational dynamics of the DENV protease.[32] In line with that are recent findings that peptide covalent inhibitors with similar structure to ours adopt two binding modes with significantly different orientations and interactions upon binding to the DENV protease.[33] The scheme of the cleavage of the inhibitor (3*S*)-**11a** is presented in Scheme 4.

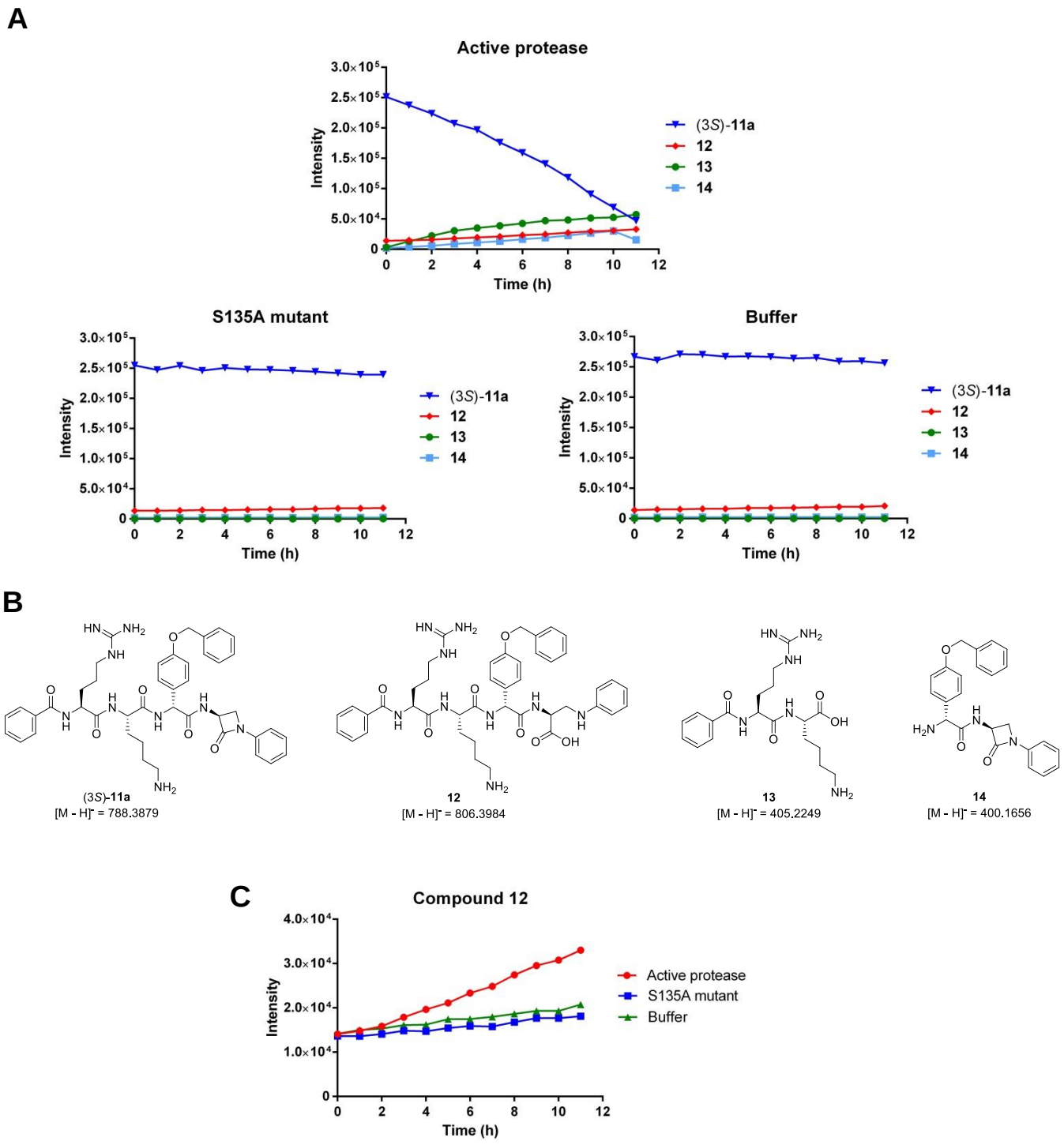

Figure 5. LC-MS measurements. **A)** Time-dependent peak intensities of the inhibitor (3*S*)-**11a** and its cleavage products **12**, **13** and **14** in mass spectra during incubation with the active DENV NS2B-NS3 protease, inactive S135A mutant and in blank incubation buffer. **B)** The structures and m/z $[M-H]^-$ ratios of compounds (3*S*)-**11a**, **12**, **13** and **14**. **C)** Comparison of time-dependent peak intensity of compound **12** during incubation of (3*S*)-**11a** with the active protease, S135A mutant and in blank incubation buffer.

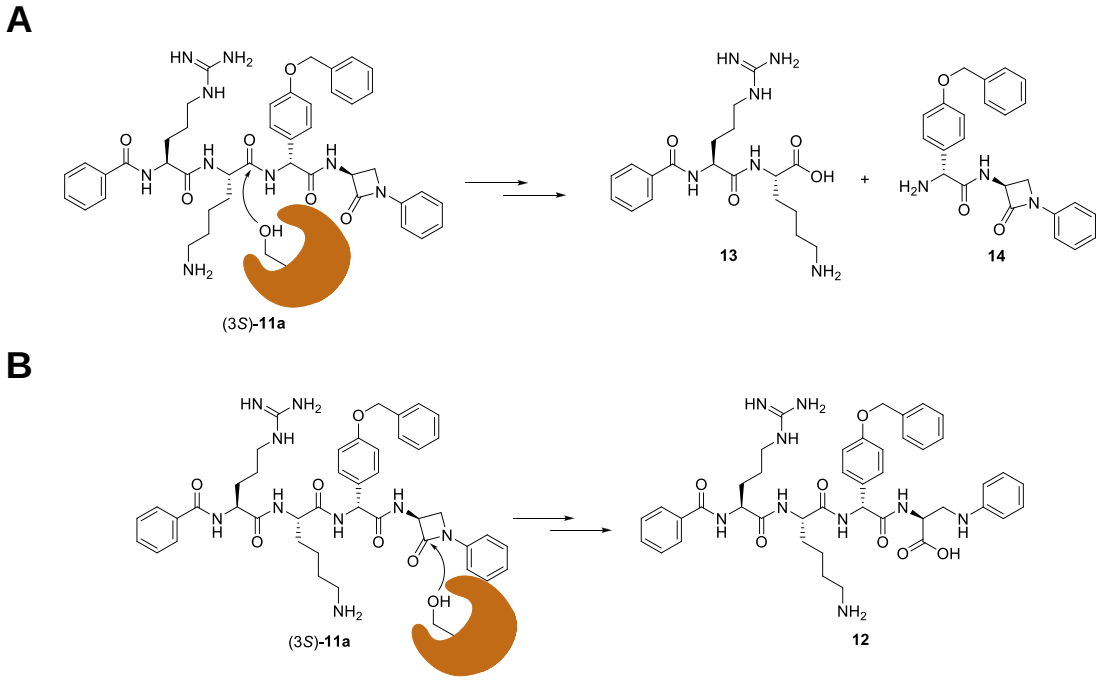

Scheme 4. Cleavage of (3*S*)-**11a** observed by LC-MS upon incubation with DENV NS2B-NS3 protease. **A)** Reaction of the catalytic serine with the lysine carbonyl group leading to the products **13** and **14**. **B)** Reaction of the catalytic serine with the β-lactam carbonyl group leading to the opening of the β-lactam ring (**12**).

The cleavage products **13** and **14** provide experimental evidence for the binding sites of the lysine and benzyloxyphenylglycine residues in DENV protease. Since the discovery of phenylglycine and benzyloxyphenylglycine as highly attractive building blocks of flaviviral protease inhibitors, there was no experimental evidence of their position within the inhibitor, while the docking results were ambiguous.[23,29,34,35] The cleavage products **13** and **14** of the inhibitor (3*S*)-**11a** indicate that lysine is positioned in the S1 site of the protease, while benzyloxyphenylglycine is placed in the prime region, occupying the S1' site and possibly extending to the S2' or S3' site. Furthermore, the incubation of the previously described tripeptide inhibitor **MB-53** (Bz-Arg-Lys-(4-benzyloxy)-D-Phg-NH_2)[23] under identical conditions resulted in similar cleavage products (*i.e.* Bz-Arg-Lys-OH and (4-benzyloxy)-D-Phg-NH_2), confirming the binding of benzyloxyphenylglycine in the prime region (Figure S9, Supporting information). The cleavage of tripeptide **MB-53** occurs faster than that of (3*S*)-**11a** (complete disappearance of the inhibitor in 7 h for **MB-53** vs. 14 h for (3*S*)-**11a**; the value for (3*S*)-**11a** was calculated from Figure 5A using linear regression). The differences in the rate of the inhibitor cleavage might be due to the influence of the β-lactam ring on the binding.

Docking studies. In order to further understand the observed binding properties and inhibition mechanism of tripeptide-β-lactam inhibitors, we performed docking studies on the compound (3*S*)-**11a** with DENV NS2B-NS3 protease as a target. For the calculations, we used crystal structure 3U1I of DENV serotype 3.[36] This structure was used as the most closely related structure to DENV serotype 2 protease in the absence of a valid crystal structure of DENV 2 protease in complex with an inhibitor. Docking results confirmed that inhibitor (3*S*)-**11a** can adopt two distinct types of conformations in the active site. The first type of conformations enables the interaction of the catalytic serine with the lysine carbonyl group, which consequently leads to the experimentally observed cleavage products **13** and **14**. The second type facilitates the interaction with β-lactam carbonyl group of the inhibitor, leading to the opening of the β-lactam ring and the product **12**. Three conformations of the first type and one conformation of the second type were found by docking studies.

In the energetically most favorable conformation of the first type, lysine is positioned in the S1 pocket and is stabilized by H-bond with Asp129 (Figure 6A and Figure S11A, Supporting information). Arginine is placed in the S2 pocket and forms H-bonds with Asp75 and Asp81 of the NS2B subunit, whereas the *N*-terminal benzoyl cap lies in the S3 hydrophobic pocket and its carbonyl group forms H-bond with Gly153 backbone. Benzyloxyphenylglycine is positioned in the prime site of the protease, with the backbone and α-C phenyl ring occupying S1' pocket and benzyloxy group extending to S2' position. The β-lactam ring is oriented from the protease towards the solvent. The other two conformations of the first type are described in detail in the Supporting information (Figures S10 and Figure S11A, Supporting information). In all three conformations, compound (3*S*)-**11a** is in appropriate orientation for nucleophilic attack of the catalytic Ser135 on the lysine carbonyl group, which leads to the cleavage of the inhibitor between lysine and benzyloxyphenylglycine and the formation of experimentally observed products **13** and **14**. The oxyanion that is formed as a result of the nucleophilic attack is in all three cases stabilized by Gly133. Furthermore, benzyloxyphenylglycine in each conformation is positioned in the prime site of the protease, which is in agreement with the experimental results.

In the second binding mode, the β-lactam ring is positioned in close proximity to the catalytic serine, with the N-1 phenyl group entering the S1 pocket (Figure 6B). In this conformation, lysine is

positioned in the S2 pocket, arginine in S3 and the *N*-terminal benzoyl cap partially occupies the S4 pocket. Arginine forms H-bond with the carbonyl oxygen of Gly153, and the benzoyl cap forms H-bond with the amino group of the same glycine (Figure S11B, Supporting information). The benzyloxyphenylglycine is again positioned in the prime site, with the backbone and the α-C phenyl ring lying in the S1' and the benzyloxy group in the S3' site. Oxyanion stabilization by Gly133 upon the nucleophilic attack of the catalytic serine on the β-lactam carbonyl group can occur in this case as well.

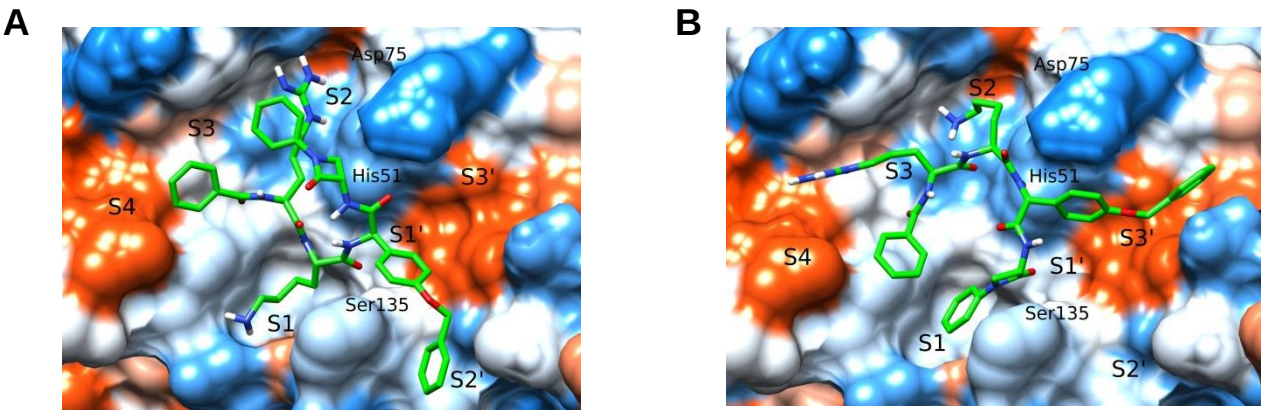

Figure 6. Results of the docking study of the compound (3*S*)-**11a** with DENV NS2B-NS3 protease as a target. **A)** Energetically most favorable conformation that enables the interaction of the catalytic serine with the lysine carbonyl group. **B)** Conformation that enables the interaction of the catalytic serine with the β-lactam carbonyl group. The protein surface is colored by amino acid property (hydrophilic - blue; hydrophobic - orange). The specificity pockets and catalytic triad are indicated.

Inhibition mechanism. In the first step, tripeptide-β-lactam inhibitors bind to the active site of DENV protease in a competitive manner. The compounds can bind in the active site in two distinct ways, placing either the lysine or the β-lactam carbonyl group in close proximity to the catalytic serine. Depending on the relative distance of each carbonyl group to the serine, a covalent interaction of one or the other carbonyl group with the serine is possible. In both cases the formation of a covalent bond proceeds through a tetrahedral oxyanion intermediate, which is stabilized by Gly133. In case of the reaction with β-lactam, this step is consistent with β-lactam inhibition of bacterial D,D-transpeptidases. However, unlike β-lactam antibiotics, here it is followed by hydrolysis of the intermediate and release of the compound with opened β-lactam ring. The hydrolysis obviously proceeds shortly after the binding as we were not able to capture the inhibitor-enzyme adduct by mass spectrometry. Rapid hydrolysis of the β-lactam-enzyme ester is quite unexpected since β-lactam antibiotics are known to form highly stable ester bonds with D,D-transpeptidases.[37] Moreover, β-lactam inhibitors of NAAA, which are structurally similar to our compounds, also irreversibly inhibit their target.[20] Reversible inhibition of β-lactams has previously been observed for ampicillin and nitrocefin in L,D-transpeptidase.[38,39] The instability of the acyl-enzyme in the former case is explained by secondary modifications of the inhibitor upon binding to the enzyme. In the latter case it is speculated that the reversible acylation is due to the very strong electron withdrawing effect of the side chain which enables the presence of negatively charged β-lactam nitrogen after ring opening. In case of β-lactam elastase inhibitors, it was observed that the absolute configuration of β-lactam plays a role in the stability of acyl-enzyme.[40] However, none of these reasons can fully explain reversible binding in our case. Unexpected reversible inhibition has also been reported for diphenyl phosphonate serine protease inhibitors.[41,42]

Antiviral activity in cellular viral replication assays. The antiviral activity of compounds (3*S*)-**11a** and (3*S*)-**11d** was tested in DENV 2 infected human hepatocarcinoma cells (Huh-7). Both compounds displayed strong reduction of virus titer with EC_{50} values 11.7 μM and 4.1 μM, respectively (Figure S12, Supporting information). The activity in cells for both compounds was in good agreement with the inhibition obtained in the biochemical assay (IC_{50} = 2.3 μM and 2.5 μM, respectively). Furthermore, both compounds showed no cytotoxicity in the concentration range 0–50 μM in the same cell line. Low cytotoxicity and high antiviral activity give these compounds a favorable selectivity index (SI).

Conclusions

In this work, we have explored the β-lactam moiety as an electrophilic warhead in flaviviral NS2B-NS3 protease inhibitors. New peptide-β-lactam inhibitors exhibited activity against the protease in both biochemical and cellular assays, with the activity of the most active inhibitors in the single-digit micromolar range. The activity of new inhibitors strongly depended on the amino acid composition, as well as on the configuration of the β-lactam ring. On the other hand, the nature of the β-lactam N-1 substituent had no influence on the activity. New inhibitors exhibited low off-target effects with almost negligible activity against thrombin and trypsin. Tripeptide-β-lactam inhibitors revealed a complex inhibition mechanism, which involves binding in the active site of the protease in two distinct conformations. One of the binding modes includes a covalent interaction of the β-lactam with the catalytic serine. The covalent interaction between the serine and the β-lactam ring is reversible and leads to the release of the inhibitor with the opened β-lactam ring. The other binding mode, which can lead to the cleavage of the amide bond between lysine and benzyloxyphenylglycine, enabled us for the first time to experimentally determine that benzyloxyphenylglycine, an amino acid that considerably contributes to the activity, binds in the prime site of the

protease. This realization might be very useful in the development of new inhibitors as it facilitates the exploration of the as-yet under-exploited prime site of the flaviviral protease for inhibitor discovery. Namely, the flaviviral protease has high preference for basic amino acids at P1 and P2 positions and therefore, it is often considered that basic amino acids are necessary to obtain high affinity of the inhibitor. However, the preference for basic amino acids at P1 and P2 positions is shared with other human serine proteases and therefore the incorporation of basic amino acids can lead to strong off-target effects. On the other hand, the prime site sequence preference is specific for flaviviral proteases. By exploiting the prime site of the protease for achieving high affinity instead of the non-prime site, basic amino acids might be replaced with non-basic amino acids. This would lead to higher selectivity, as well as an improvement of pharmacokinetic properties. It is encouraging that our new inhibitors showed high selectivity, which is a frequent shortfall of electrophilic warheads, as well as strong activity in cells combined with low cytotoxicity. Further efforts should be made in finding an optimal position of the β-lactam within the inhibitor to enable exclusive, and possibly irreversible, binding of the β-lactam carbonyl group to the catalytic serine. The β-lactam moiety as an electrophilic warhead provides a great variation in the choice of substituents as well as spatial arrangement of the ring, which can be used to optimize and fine-tune the properties of an inhibitor.

Experimental section

General comments. All chemicals and solvents were purchased from commercial suppliers and were used without further purification. THF was stored on molecular sieves. All final di- and tripeptide-β-lactam derivatives had purity > 95% determined by HPLC. Flash column chromatography was performed on the Biotage Isolera One purification system with the silica gel filled commercial cartridges (mesh 230-400, 60 Å). Products were detected by UV monitoring at 254 and 280 nm. NMR spectra were measured on Varian NMR instrument at 300 or 500 MHz at room temperature. $CDCl_3$, DMSO-d_6 or CD_3OD were used as solvents. Chemical shifts (δ) are given in ppm relative to residual nondeuterated solvent peaks as internal standard. HR-ESI mass spectra were obtained on a Bruker microTOF-Q II mass spectrometer. The final di- and tripeptide-β-lactam derivatives were purified by preparative HPLC on an ÄKTA Purifier system (GE Healthcare, Germany) using a RP-18 pre- and main column (Reprospher 100 C-18-DE, Dr. Maisch GmbH, Germany, 5 µm, precolumn 30 × 16 mm, main column 125 × 16 mm). Method used for the purification was as follows: eluent A - water (0.1% TFA), eluent B - methanol (0.1% TFA): 0 - 2.5 min 10% B; 2.6 min - 23.5 min gradient 10% B -100% B, 23.6 min - 26.0 min 100% B, 26.1 min - 30.0 min 10% B; flow rate 8 mL/min; λ = 214, 254, 280 nm. Purity of final compounds and the ratio of epimers in tripeptide-β-lactam derivatives were analyzed on an analytical Jasco HPLC system equipped with UV/Vis detector with RP-18 column (Reprosil-Pur ODS-3, Dr. Maisch GmbH, Germany, 5 µm, 50 × 2 mm). Samples for the analysis were prepared by adding 2.5 µL of the 10 mM Stock solution of the compound in DMSO to 100 µL water/acetonitrile 1 : 1 solution. The method for the purity determination was: eluent A - water (0.1% TFA), eluent B - acetonitrile (0.1% TFA): 0 - 0.2 min 1% B; 0.3 min - 7.0 min gradient 1% B - 100% B, 7.1 min - 8.0 min 100% B, 8.1 min - 9.6 min 1% B; flow rate 1 mL/min; λ = 254 nm, injected volume: 10 µL. For the analysis of the ratio of epimers the method was: eluent A - water (0.1% TFA), eluent B - acetonitrile (0.1% TFA): 0 - 0.2 min 1% B; 0.3 min - 27.0 min gradient 1% B - 100% B, 27.1 min - 28.0 min 100% B, 28.1 min - 30.0 min 1% B; flow rate 1 mL/min; λ = 254 nm, injected volume: 10 µL. Compound **9** was synthesized as previously described.[23] The biochemical assays and dilution experiment were measured on a BMG Labtech Fluostar OPTIMA microtiter fluorescence plate reader (BMG Labtech, Germany). Tryptophan quenching assays were measured on Tecan Safire II instrument (Tecan Group Ltd., Switzerland).

Synthesis of dipeptide-β-lactam derivatives. Derivatives (3*R*)- and (3*S*)-**4**–**8** were synthesized using the mixed-anhydride method. The corresponding β-lactam (1.0 equiv) was dissolved in THF (2 mL) in the reaction flask and NMM (1.1 equiv) was added. Corresponding protected dipeptide (1.0 equiv.) was dissolved in THF (2 mL) in a separate flask, NMM (1.1 equiv) was added and the temperature was decreased to -15 °C. IBCF (1.0 equiv) was added to the peptide solution and the mixture was stirred for 5 minutes. The peptide solution was added dropwise to the reaction flask and the reaction proceeded for 30 minutes at -15 °C and further 16 h at room temperature. The reaction mixture was evaporated to dryness. Boc and Pbf protection groups were cleaved without purification of the obtained product using dichloromethane : TFA 1 : 1 (total volume 1.5 mL). The reaction proceeded for 2 h at room temperature, after which the reaction mixture was evaporated to dryness. The product was purified by preparative HPLC.

Bz-Arg-Lys-(3*R*)-3-amino-1-phenylazetidin-2-one ((3*R*)-4). Obtained as white powder (13 mg, 62%) from dipeptide Bz-Arg(Pbf)-Lys(Boc)-OH (28 mg, 37 µmol) and β-lactam (3*R*)-**3a** (7 mg, 37 µmol). ^{1}H NMR (500 MHz, CD_3OD) δ 7.85 (d, J = 7.2 Hz, 2H), 7.56 (t, J = 7.4 Hz, 1H), 7.47 (t, J = 7.6 Hz, 2H), 7.41–7.36 (m, 4H), 7.15 (t, J = 7.0 Hz, 1H), 5.06 (dd, J = 5.6, 2.7 Hz, 1H), 4.57–4.50 (m, 1H), 4.43 (dd, J = 9.0, 5.5 Hz, 1H), 4.03 (t, J = 5.7 Hz, 1H), 3.72 (dd, J = 5.7, 2.7 Hz, 1H), 3.25 (t, J = 7.1 Hz, 2H), 2.93 (t, J = 7.5 Hz, 2H), 2.02–1.63 (m, 8H), 1.58–1.46 (m, 2H). ^{13}C NMR (126 MHz, CD_3OD) δ 174.3, 174.2, 170.6, 166.2, 158.6, 139.4, 135.0, 133.1, 130.3, 129.6, 128.5, 125.6, 117.8, 56.4, 55.1, 54.2, 47.7, 42.1, 40.5, 32.4, 29.8, 28.0, 26.4, 23.7. HRMS (ESI): m/z $[M + H]^+$ calcd for $C_{28}H_{39}N_8O_4$, 551.3089; found, 551.3072.

Bz-Arg-Lys-(3*S*)-3-amino-1-phenylazetidin-2-one ((3*S*)-4). Obtained as white powder (12 mg, 50%) from dipeptide Bz-Arg(Pbf)-Lys(Boc)-OH (32 mg, 41 µmol) and β-lactam (3*S*)-**3a** (8 mg, 41 µmol). ^{1}H NMR (500 MHz, CD_3OD) δ 7.88–7.80 (m, 2H), 7.55 (t, J = 7.4 Hz, 1H), 7.45 (t, J = 7.7 Hz, 2H), 7.42–7.33 (m, 4H), 7.14 (t, J = 7.1 Hz, 1H), 5.01 (dd, J = 5.7, 2.7 Hz, 1H), 4.51 (dd, J = 8.1, 6.3 Hz, 1H), 4.44 (dd, J = 9.0, 5.3 Hz, 1H), 4.02 (t, J = 5.7 Hz, 1H), 3.77 (dd, J = 5.6, 2.8 Hz, 1H), 3.23 (t, J = 7.0 Hz, 2H), 2.93 (t, J = 7.5 Hz, 2H), 1.99–1.84 (m, 3H), 1.82–1.63 (m, 5H), 1.57–1.46 (m, 2H). ^{13}C NMR (126 MHz, CD_3OD) δ 174.36, 174.27, 170.6, 166.2, 158.6, 139.4, 135.0, 133.1, 130.3, 129.6, 128.5, 125.5, 117.8, 56.5, 55.2, 54.1, 47.4, 42.0, 40.5, 32.3, 29.8, 28.0, 26.4, 23.6. HRMS (ESI): m/z $[M + H]^+$ calcd for $C_{28}H_{39}N_8O_4$, 551.3089; found, 551.3071.

Bz-Lys-Lys-(3*R*)-3-amino-1-phenylazetidin-2-one ((3*R*)-5). Obtained as white powder (11 mg, 34%) from dipeptide Bz-Lys(Boc)-Lys(Boc)-OH (38 mg, 65 µmol) and β-lactam (3*R*)-**3a** (13 mg, 65 µmol). ^{1}H NMR (500 MHz, CD_3OD) δ 7.86 (d, J = 7.3 Hz, 2H), 7.55 (t, J = 7.4 Hz, 1H), 7.46 (t, J = 7.7 Hz, 2H), 7.43–7.34 (m, 4H), 7.14 (t, J = 7.1 Hz, 1H), 5.05 (dd, J = 5.6, 2.7 Hz,

1H), 4.49 (t, *J* = 7.3 Hz, 1H), 4.43 (dd, *J* = 9.1, 5.3 Hz, 1H), 4.02 (t, *J* = 5.7 Hz, 1H), 3.72 (dd, *J* = 5.7, 2.8 Hz, 1H), 2.97 (t, *J* = 7.4 Hz, 2H), 2.93 (t, *J* = 7.5 Hz, 2H), 2.01–1.64 (m, 8H), 1.61–1.43 (m, 4H). ^{13}C NMR (126 MHz, CD_3OD) *δ* 174.44, 174.37, 170.6, 166.2, 139.4, 135.0, 133.0, 130.3, 129.6, 128.5, 125.5, 117.8, 56.4, 55.5, 54.2, 47.6, 40.56, 40.51, 32.4, 32.1, 28.2, 28.0, 23.9, 23.7. HRMS (ESI): *m/z* $[M + H]^+$ calcd for $C_{28}H_{39}N_6O_4$, 523.3027; found, 523.3037

Bz-Lys-Lys-(3*S*)-3-amino-1-phenylazetidin-2-one ((3*S*)-5). Obtained as white powder (13 mg, 40%) from dipeptide Bz-Lys(Boc)-Lys(Boc)-OH (35 mg, 60 μmol) and β-lactam (3*S*)-**3a** (12 mg, 60 μmol). ^{1}H NMR (500 MHz, CD_3OD) *δ* 7.91–7.79 (m, 2H), 7.55 (t, *J* = 7.4 Hz, 1H), 7.47–7.34 (m, 6H), 7.14 (t, *J* = 7.1 Hz, 1H), 5.02 (dd, *J* = 5.6, 2.7 Hz, 1H), 4.53–4.46 (m, 2H), 4.44 (dd, *J* = 9.0, 5.3 Hz, 1H), 4.02 (t, *J* = 5.7 Hz, 1H), 3.78 (dd, *J* = 5.6, 2.8 Hz, 1H), 2.98–2.90 (m, 4H), 2.00–1.83 (m, 3H), 1.82–1.62 (m, 5H), 1.61–1.43 (m, 4H). ^{13}C NMR (126 MHz, CD_3OD) *δ* 174.5, 174.4, 170.6, 166.2, 139.4, 135.0, 133.0, 130.3, 129.6, 128.6, 125.5, 117.8, 56.5, 55.6, 54.1, 47.4, 40.54, 40.50, 32.3, 32.0, 28.2, 28.0, 24.0, 23.6. HRMS (ESI): *m/z* $[M + H]^+$ calcd for $C_{28}H_{39}N_6O_4$, 523.3027; found, 523.3008.

Bz-Lys-Arg-(3*R*)-3-amino-1-phenylazetidin-2-one ((3*R*)-6). Obtained as white powder (6 mg, 28%) from dipeptide Bz-Lys(Boc)-Arg(Pbf)-OH (27 mg, 36 μmol) and β-lactam (3*R*)-**3a** (7 mg, 36 μmol). ^{1}H NMR (500 MHz, CD_3OD) *δ* 7.88–7.82 (m, 2H), 7.56 (t, *J* = 7.4 Hz, 1H), 7.46 (t, *J* = 7.7 Hz, 2H), 7.43–7.34 (m, 4H), 7.17–7.13 (m, 1H), 5.05 (dd, *J* = 5.6, 2.7 Hz, 1H), 4.53–4.48 (m, 1H), 4.44 (dd, *J* = 8.6, 5.4 Hz, 1H), 4.02 (t, *J* = 5.7 Hz, 1H), 3.72 (dd, *J* = 5.8, 2.8 Hz, 1H), 3.22 (t, *J* = 7.1 Hz, 2H), 2.97 (t, *J* = 7.5 Hz, 2H), 2.01–1.63 (m, 8H), 1.62–1.44 (m, 2H). ^{13}C NMR (126 MHz, CD_3OD) *δ* 174.4, 174.1, 170.6, 166.1, 158.7, 139.4, 135.1, 133.0, 130.3, 129.6, 128.5, 125.5, 117.8, 56.4, 55.4, 54.1, 47.6, 42.0, 40.6, 32.1, 30.2, 28.2, 26.3, 23.9. HRMS (ESI): *m/z* $[M + H]^+$ calcd for $C_{28}H_{39}N_8O_4$, 551.3089; found, 551.3096.

Bz-Lys-Arg-(3*S*)-3-amino-1-phenylazetidin-2-one ((3*S*)-6). Obtained as white powder (3 mg, 15%) from dipeptide Bz-Lys(Boc)-Arg(Pbf)-OH (27 mg, 35 μmol) and β-lactam (3*S*)-**3a** (7 mg, 35 μmol). ^{1}H NMR (500 MHz, CD_3OD) *δ* 7.84 (d, *J* = 7.3 Hz, 2H), 7.55 (t, *J* = 7.5 Hz, 1H), 7.44 (t, *J* = 7.7 Hz, 3H), 7.42–7.34 (m, 4H), 5.02 (dd, *J* = 5.8, 2.8 Hz, 1H), 4.50 (dd, *J* = 8.3, 6.4 Hz, 1H), 4.45 (dd, *J* = 8.3, 5.4 Hz, 1H), 4.03 (t, *J* = 5.7 Hz, 1H), 3.77 (dd, *J* = 5.7, 2.8 Hz, 1H), 3.22 (t, *J* = 7.0 Hz, 2H), 2.95 (t, *J* = 7.5 Hz, 2H), 2.00–1.84 (m, 3H), 1.82–1.65 (m, 4H), 1.64–1.45 (m, 3H). ^{13}C NMR (126 MHz, CD_3OD) *δ* 174.5, 174.1, 170.6, 166.1, 158.6, 139.4, 135.0, 133.0, 130.3, 129.6, 128.5, 125.5, 117.8, 56.5, 55.5, 54.0, 47.4, 42.0, 40.6, 32.1, 30.1, 28.2, 26.2, 24.0. HRMS (ESI): *m/z* $[M + H]^+$ calcd for $C_{28}H_{39}N_8O_4$, 551.3089; found, 551.3104.

Bz-Lys-Nle-(3*R*)-3-amino-1-phenylazetidin-2-one ((3*R*)-7). Obtained as white powder (4 mg, 12%) from dipeptide Bz-Lys(Boc)-Nle-OH (31 mg, 66 μmol) and β-lactam (3*R*)-**3a** (13 mg, 66 μmol). ^{1}H NMR (500 MHz, CD_3OD) δ 7.89–7.81 (m, 2H), 7.55 (t, *J* = 7.4 Hz, 1H), 7.45 (t, *J* = 7.7 Hz, 2H), 7.42–7.34 (m, 4H), 7.14 (t, *J* = 7.1 Hz, 1H), 5.03 (dd, *J* = 5.6, 2.7 Hz, 1H), 4.57 (t, *J* = 7.2 Hz, 1H), 4.36 (dd, *J* = 8.8, 5.6 Hz, 1H), 4.00 (t, *J* = 5.7 Hz, 1H), 3.69 (dd, *J* = 5.7, 2.7 Hz, 1H), 2.96 (t, *J* = 7.4 Hz, 2H), 2.00–1.92 (m, 1H), 1.89–1.80 (m, 2H), 1.76–1.68 (m, 3H), 1.57–1.48 (m, 2H), 1.43–1.31 (m, 4H), 0.91 (t, *J* = 7.0 Hz, 3H). ^{13}C NMR (126 MHz, CD_3OD) δ 174.8, 174.1, 170.4, 166.1, 139.4, 135.1, 133.0, 130.3, 129.6, 128.5, 125.4, 117.8, 56.5, 55.0, 54.8, 47.7, 40.6, 32.7, 32.3, 29.1, 28.2, 23.8, 23.4, 14.2. HRMS (ESI): *m/z* $[M + H]^+$ calcd for $C_{28}H_{38}N_5O_4$, 508.2918; found, 508.2921.

Bz-Lys-Nle-(3*S*)-3-amino-1-phenylazetidin-2-one ((3*S*)-7). Obtained as white powder (4 mg, 12%) from dipeptide Bz-Lys(Boc)-Nle-OH (27 mg, 58 μmol) and β-lactam (3*S*)-**3a** (11 mg, 58 μmol). ^{1}H NMR (500 MHz, CD_3OD) *δ* 7.87–7.81 (m, 2H), 7.54 (t, *J* = 7.4 Hz, 1H), 7.50–7.34 (m, 6H), 7.14 (m, 1H), 5.06 (dd, *J* = 5.7, 2.8 Hz, 1H), 4.56 (dd, *J* = 7.9, 6.5 Hz, 1H), 4.36 (dd, *J* = 9.0, 5.5 Hz, 1H), 4.03 (t, *J* = 5.8 Hz, 1H), 3.75–3.72 (m, 1H), 2.94 (t, *J* = 7.5 Hz, 2H), 1.99–1.91 (m, 1H), 1.88–1.80 (m, 2H), 1.75–1.66 (m, 3H), 1.57–1.47 (m, 2H), 1.44–1.31 (m, 4H), 0.91 (t, *J* = 7.0 Hz, 3H). ^{13}C NMR (126 MHz, CD_3OD) *δ* 174.8, 174.2, 170.4, 166.0, 139.5, 135.0, 133.0, 130.3, 129.6, 128.5, 125.5, 117.8, 56.4, 55.1, 54.7, 47.5, 40.6, 32.7, 32.3, 29.1, 28.1, 23.8, 23.4, 14.2. HRMS (ESI): *m/z* $[M + H]^+$ calcd for $C_{28}H_{39}N_5O_4$, 508.2918; found, 508.2913.

Bz-Arg-Nle-(3*R*)-3-amino-1-phenylazetidin-2-one ((3*R*)-8). Obtained as white powder (5 mg, 18%) from dipeptide Bz-Arg(Pbf)-Nle-OH (31 mg, 48 μmol) and β-lactam (3*R*)-**3a** (9 mg, 48 μmol). ^{1}H NMR (500 MHz, CD_3OD) *δ* 7.85 (d, *J* = 7.4 Hz, 2H), 7.55 (t, *J* = 7.4 Hz, 1H), 7.46 (t, *J* = 7.7 Hz, 2H), 7.42–7.30 (m, 4H), 7.14 (t, *J* = 7.1 Hz, 1H), 5.03 (dd, *J* = 5.5, 2.6 Hz, 1H), 4.62 (t, *J* = 7.0 Hz, 1H), 4.36 (dd, *J* = 8.7, 5.5 Hz, 1H), 4.01 (t, *J* = 5.6 Hz, 1H), 3.71 (dd, *J* = 5.7, 2.7 Hz, 1H), 3.24 (t, *J* = 6.9 Hz, 2H), 2.01–1.93 (m, 1H), 1.91–1.78 (m, 2H), 1.76–1.64 (m, 3H), 1.45–1.26 (m, 4H), 0.92 (t, *J* = 6.8 Hz, 3H). ^{13}C NMR (126 MHz, CD_3OD) δ 174.8, 173.9, 170.3, 166.1, 158.6, 139.4, 135.0, 133.0, 130.3, 129.6, 128.5, 125.5, 117.8, 56.5, 54.8, 54.6, 47.6, 42.0, 32.7, 30.1, 29.1, 26.2, 23.4, 14.2. HRMS (ESI): *m/z* $[M + H]^+$ calcd for $C_{28}H_{38}N_7O_4$, 536.2980; found, 536.2984.

Bz-Arg-Nle-(3*S*)-3-amino-1-phenylazetidin-2-one ((3*S*)-8). Obtained as white powder (9 mg, 26%) from dipeptide Bz-Arg(Pbf)-Nle-OH (38 mg, 59 μmol) and β-lactam (3*S*)-**3a** (12 mg, 59 μmol). ^{1}H NMR (500 MHz, CD_3OD) *δ* 7.88–7.82 (m, 2H), 7.54 (t, *J* = 7.4 Hz, 1H), 7.51–7.33 (m, 6H), 7.14 (t, *J* = 7.1 Hz, 1H), 5.04 (dd, *J* = 5.7, 2.8 Hz, 1H), 4.59 (dd, *J* = 7.7, 6.3 Hz, 1H), 4.36 (dd, *J* = 9.0, 5.4 Hz, 1H), 4.02 (t, *J* = 5.7 Hz, 1H), 3.75–3.72 (m, 1H), 3.21 (t, *J* = 7.1 Hz, 2H), 2.01–1.92 (m, 1H), 1.90–1.81 (m, 2H), 1.76–1.66 (m, 3H), 1.43–1.29 (m, 4H), 0.92 (t, *J* = 7.1 Hz, 3H). ^{13}C NMR (126 MHz, CD_3OD) *δ* 174.8, 174.1, 170.4, 166.1, 158.6, 139.4, 135.0, 133.0, 130.3, 129.6, 128.5, 125.5, 117.8, 56.5, 54.8, 54.7, 47.6, 42.0, 32.7, 30.0, 29.1, 26.2, 23.4, 14.2. HRMS (ESI): *m/z* $[M + H]^+$ calcd for $C_{28}H_{38}N_7O_4$, 536.2980; found, 536.2988.

General procedure for the coupling of β-lactams to Fmoc-protected 4-benzyloxyphenylglycine. Fmoc-protected 4-benzyloxy-D-Phg **9** (1.0 equiv) was dissolved in DMF (2 mL) in the reaction flask. Corresponding β-lactam (1.0 equiv) was dissolved in DMF (2 mL) in a separate flask. TMP (1.1 equiv) was added to each flask, after which the β-lactam solution was transferred into the reaction flask. The temperature was decreased to 0 °C and COMU (1.1 equiv) was added. The reaction proceeded at 0 °C for 1 h and additional 3 h at room temperature. Ethyl acetate (30 mL) was added and the solution was washed with 1 M HCl (2 × 25 mL), saturated $NaHCO_3$ (2 × 25 mL) and saturated NaCl solution (2 × 25 mL). The organic layer was dried with $MgSO_4$ and

evaporated to dryness. The crude Fmoc-protected product was dissolved in a solution of 25% piperidine in DMF (5 mL) and the reaction mixture was stirred at room temperature for 15 min. Ethyl acetate (30 mL) was added and the resulting solution was washed with deionized water (2 × 25 mL). The organic phase was dried with $MgSO_4$ and evaporated to dryness. The crude product was purified by silica gel column chromatography (ethyl acetate/methanol, gradient).

(*R*)-2-amino-2-(4-(benzyloxy)phenyl)-*N*-((*R*)-2-oxo-1-phenylazetidin-3-yl)acetamide ((3*R*)-10a). Obtained as yellow solid (22 mg, 28%) from (3*R*)-**3a** (38 mg, 0.19 mmol) and protected amino acid **9** (92 mg, 0.19 mmol) with addition of COMU (90 mg, 0.21 mmol) and TMP (56 µL, 0.42 mmol). ^{1}H NMR (300 MHz, DMSO-d_6) δ 8.82 (br s, 1H), 7.42–7.30 (m, 11H), 7.10 (br s, 1H), 6.96 (d, J = 7.4 Hz, 2H), 5.09 (s, 2H), 5.01 (br s, 1H), 4.35 (s, 1H), 3.92–3.89 (m, 1H), 3.53 (br s, 1H). ^{13}C NMR (75 MHz, DMSO-d_6) δ 173.7, 164.6, 157.6, 138.1, 137.2, 134.1, 129.2, 128.4, 127.96, 127.77, 127.59, 123.6, 116.1, 114.5, 69.2, 58.2, 54.8, 46.2. HRMS (ESI) m/z [M + H]$^+$ calcd for $C_{24}H_{24}N_3O_3$, 402.1812; found, 402.1794.

(*R*)-2-amino-2-(4-(benzyloxy)phenyl)-*N*-((*S*)-2-oxo-1-phenylazetidin-3-yl)acetamide ((3*S*)-10a). Obtained as white solid (45 mg, 44%) from (3*S*)-**3a** (50 mg, 0.25 mmol) and protected amino acid **9** (121 mg, 0.25 mmol) with addition of COMU (119 mg, 0.28 mmol) and TMP (73 µL, 0.55 mmol). ^{1}H NMR (300 MHz, DMSO-d_6) δ 8.80 (br s, 1H), 7.45–7.29 (m, 11H), 7.13–7.06 (m, 1H), 6.96 (d, J = 8.7 Hz, 2H), 5.09 (s, 2H), 4.99 (br s, 1H), 4.32 (s, 1H), 3.90 (t, J = 5.7 Hz, 1H), 3.57 (dd, J = 5.7, 2.9 Hz, 1H). ^{13}C NMR (75 MHz, DMSO-d_6) δ 173.9, 164.7, 157.5, 138.2, 137.2, 134.6, 129.2, 128.4, 127.91, 127.75, 127.58, 123.57, 116.1, 114.4, 69.1, 58.4, 54.8, 46.2. HRMS (ESI) m/z [M + H]$^+$ calcd for $C_{24}H_{24}N_3O_3$, 402.1812; found 402.1823.

(*R*)-2-amino-2-(4-(benzyloxy)phenyl)-*N*-((*R*)-2-oxo-1-(4-methylphenyl)azetidin-3-yl)acetamide ((3*R*)-10b). Obtained as a yellow solid (31 mg, 35%) from (3*R*)-**3b** (45 mg, 0.21 mmol) and protected amino acid **9** (101 mg, 0.21 mmol) with addition of COMU (100 mg, 0.23 mmol) and TMP (62 µL, 0.46 mmol). ^{1}H NMR (300 MHz, DMSO-d_6) δ 8.80 (br s, 1H), 7.45–7.16 (m, 11H), 6.97 (t, J = 8.9 Hz, 2H), 5.09 (s, 2H), 5.00 (br s, 1H), 4.31 (s, 1H), 3.86 (t, J = 5.6 Hz, 1H), 3.49 (dd, J = 5.6, 2.5 Hz, 1H), 2.26 (s, 3H). ^{13}C NMR (75 MHz, DMSO-d_6) δ 174.0, 164.3, 157.5, 137.2, 135.8, 134.6, 132.6, 129.5, 128.4, 127.85, 127.75, 127.58, 116.1, 114.4, 69.1, 58.4, 54.8, 46.2, 20.5. HRMS (ESI) m/z [M + H]$^+$ calcd for $C_{25}H_{25}N_3O_3$, 416.1969; found, 416.1964.

(*R*)-2-amino-2-(4-(benzyloxy)phenyl)-*N*-((*S*)-2-oxo-1-(4-methylphenyl)azetidin-3-yl)acetamide ((3*S*)-10b). Obtained as a yellow solid (38 mg, 39%) from (3*S*)-**3b** (50 mg, 0.24 mmol) and protected amino acid **9** (113 mg, 0.24 mmol) with addition of COMU (111 mg, 0.26 mmol) and TMP (68 µL, 0.52 mmol). ^{1}H NMR (300 MHz, DMSO-d_6) δ 8.80 (br s, 1H), 7.47–7.14 (m, 11H), 6.96 (t, J = 8.4 Hz, 2H), 5.09 (s, 2H), 4.99 (br s, 1H), 4.32 (s, 1H), 3.87 (t, J = 5.6 Hz, 1H), 3.54 (dd, J = 5.4, 2.7 Hz, 1H), 2.27 (s, 3H). ^{13}C NMR (75 MHz, DMSO-d_6) δ 174.0, 164.4, 157.5, 137.2, 135.8, 134.7, 132.7, 129.5, 128.4, 127.92, 127.78, 127.60, 116.1, 114.5, 69.2, 58.4, 54.8, 46.2, 20.5. HRMS (ESI) m/z [M + H]$^+$ calcd for $C_{25}H_{26}N_3O_3$, 416.1969; found, 416.1955.

(*R*)-2-amino-2-(4-(benzyloxy)phenyl)-*N*-((*R*)-2-oxo-1-(3-methylphenyl)azetidin-3-yl)acetamide ((3*R*)-10c). Obtained as an off-white solid (65 mg, 50%) from (3*R*)-**3c** (67 mg, 0.31 mmol) and protected amino acid **9** (150 mg, 0.31 mmol) with addition of COMU (147 mg, 0.34 mmol) and TMP (90 µL, 0.69 mmol). ^{1}H NMR (300 MHz, DMSO-d_6) δ 8.79 (br s, 1H), 7.45–7.13 (m, 10H), 6.96–6.90 (m, 3H), 5.08 (s, 2H), 4.99 (br s, 1H), 4.31 (s, 1H), 3.87 (t, J = 5.6 Hz, 1H), 3.51 (dd, J = 5.1, 2.6 Hz, 1H), 2.29 (s, 3H). ^{13}C NMR (75 MHz, DMSO-d_6) δ 174.0, 164.6, 157.5, 138.6, 138.1, 137.2, 134.6, 129.0, 128.4, 127.86, 127.76, 127.6, 124.3, 116.5, 114.4, 113.4, 69.1, 58.4, 54.7, 46.2, 21.1. HRMS (ESI) m/z [M + H]$^+$ calcd for $C_{25}H_{25}N_3O_3$, 416.1969; found, 416.1968.

(*R*)-2-amino-2-(4-(benzyloxy)phenyl)-*N*-((*S*)-2-oxo-1-(3-methylphenyl)azetidin-3-yl)acetamide ((3*S*)-10c). Obtained as an off-white solid (59 mg, 45%) from (3*S*)-**3c** (67 mg, 0.31 mmol) and protected amino acid **9** (150 mg, 0.31 mmol) with addition of COMU (147 mg, 0.34 mmol) and TMP (90 µL, 0.69 mmol). ^{1}H NMR (300 MHz, DMSO-d_6) δ 8.79 (br s, 1H), 7.45–7.13 (m, 10H), 6.99–6.90 (m, 3H), 5.09 (s, 2H), 4.97 (br s, 1H), 4.31 (s, 1H), 3.88 (t, J = 5.6 Hz, 1H), 3.55 (dd, J = 5.0, 2.6 Hz, 1H), 2.29 (s, 3H). ^{13}C NMR (75 MHz, DMSO-d_6) δ 174.0, 164.7, 157.5, 138.6, 138.2, 137.2, 134.7, 129.0, 128.4, 127.91, 127.76, 127.6, 124.3, 116.5, 114.4, 113.4, 69.2, 58.4, 54.8, 46.2, 21.1. HRMS (ESI) m/z [M + H]$^+$ calcd for $C_{25}H_{26}N_3O_3$, 416.1969; found, 416.1957.

(*R*)-2-amino-2-(4-(benzyloxy)phenyl)-*N*-((*R*)-2-oxo-1-(4-fluorophenyl)azetidin-3-yl)acetamide ((3*R*)-10d). Obtained as a yellow solid (25 mg, 26%) from (3*R*)-**3d** (49 mg, 0.23 mmol) and protected amino acid **9** (111 mg, 0.23 mmol) with addition of COMU (109 mg, 0.25 mmol) and TMP (67 µL, 0.51 mmol). ^{1}H NMR (300 MHz, DMSO-d_6) δ 8.80 (br s, 1H), 7.47–7.18 (m, 11H), 6.95 (d, J = 8.4 Hz, 2H), 5.09 (s, 2 H), 5.01 (br s, 1 H), 4.32 (s, 1H), 3.89 (t, J = 5.5 Hz, 1H), 3.53 (dd, J = 5.9 Hz, 2.6 Hz, 1H). ^{13}C NMR (75 MHz, DMSO-d_6) δ 174.0, 164.4, 158.1 (d, J = 237.6 Hz), 157.5, 137.2, 134.7 (d, J = 2.7 Hz), 134.5, 128.4, 127.89, 127.76, 127.59, 117.8 (d, J = 7.8 Hz), 115.9 (d, J = 22.7 Hz), 114.4, 69.1, 58.3, 55.0, 46.4. HRMS (ESI) m/z [M + H]$^+$ calcd for $C_{24}H_{23}FN_3O_3$, 420.1718; found, 420.1707.

(*R*)-2-amino-2-(4-(benzyloxy)phenyl)-*N*-((*S*)-2-oxo-1-(4-fluorophenyl)azetidin-3-yl)acetamide ((3*S*)-10d). Obtained as a yellow solid (45 mg, 43%) from (3*S*)-**3d** (53 mg, 0.25 mmol) and protected amino acid **9** (117 mg, 0.25 mmol) with addition of COMU (115 mg, 0.27 mmol) and TMP (72 µL, 0.54 mmol). ^{1}H NMR (300 MHz, dmso) δ 8.80 (br s, 1H), 7.51–7.16 (m, 11H), 6.97 (t, J = 8.0 Hz, 2H), 5.09 (s, 2H), 5.00 (br s, 1H), 4.32 (s, 1H), 3.89 (t, J = 5.6 Hz, 1H), 3.57 (dd, J = 5.3, 2.8 Hz, 1H). ^{13}C NMR (75 MHz, DMSO-d_6) δ 174.0, 164.5, 158.1 (d, J = 240.5 Hz), 157.5, 137.2, 134.77 (d, J = 2.3 Hz), 134.66, 128.4, 127.90, 127.76, 127.6, 117.8 (d, J = 7.8 Hz), 115.9 (d, J = 22.8 Hz), 114.4, 69.2, 58.4, 55.0, 46.4. HRMS (ESI) m/z [M + Na]$^+$ calcd for $C_{24}H_{22}FN_3NaO_3$, 442.1537; found, 442.1530.

(*R*)-2-amino-2-(4-(benzyloxy)phenyl)-*N*-((*R*)-2-oxo-1-(3-fluorophenyl)azetidin-3-yl)acetamide ((3*R*)-10e). Obtained as a yellow solid (14 mg, 23%) from (3*R*)-**3e** (32 mg, 0.15 mmol) and protected amino acid **9** (71 mg, 0.15 mmol) with addition of COMU (70 mg, 0.16 mmol) and TMP (42 µL, 0.32 mmol). ^{1}H NMR (300 MHz, DMSO-d_6) δ 8.80 (br s, 1H), 7.45–7.27 (m, 8H), 7.19 (t, J = 7.2 Hz, 2H), 6.99–6.92 (m, 3H), 5.09 (s, 2H), 5.01 (br s, 1H), 4.31 (s, 1H), 3.91 (t, J = 5.6 Hz, 1H), 3.56 (dd, J = 5.6, 3.0 Hz, 1H). ^{13}C NMR (75 MHz, DMSO-d_6) δ 174.1,

165.1, 162.4 (d, J = 247.6 Hz), 157.5, 139.6 (d, J = 10.8 Hz), 137.2, 134.5, 131.1 (d, J = 9.8 Hz), 128.4, 127.89, 127.76, 127.59, 114.4, 112.2 (d, J = 2.6 Hz), 110.2 (d, J = 21.3 Hz), 103.3 (d, J = 25.8 Hz), 69.2, 58.4, 55.1, 46.6. HRMS (ESI) m/z $[M + H]^+$ calcd for $C_{24}H_{23}FN_3O_3$, 420.1718; found, 420.1707.

(*R*)-2-amino-2-(4-(benzyloxy)phenyl)-*N*-((*S*)-2-oxo-1-(3-fluorophenyl)azetidin-3-yl)acetamide ((3*S*)-10e). Obtained as a yellow solid (47 mg, 47%) from (3*S*)-**3e** (51 mg, 0.24 mmol) and protected amino acid **9** (113 mg, 0.24 mmol) with addition of COMU (111 mg, 0.26 mmol) and TMP (68 μL, 0.52 mmol). ^{1}H NMR (300 MHz, DMSO-d_6) δ 8.80 (s, 1H), 7.52–7.24 (m, 8H), 7.18 (d, J = 8.5 Hz, 2H), 7.02–6.88 (m, 3H), 5.09 (s, 2H), 5.00 (br s, 1H), 4.32 (s, 1H), 3.91 (t, J = 5.6 Hz, 1H), 3.59 (dd, J = 4.6, 2.7 Hz, 1H). ^{13}C NMR (75 MHz, DMSO-d_6) δ 174.1, 165.1, 162.4 (d, J = 245.6 Hz), 157.5, 139.6 (d, J = 10.8 Hz), 137.2, 134.6, 131.1 (d, J = 9.6 Hz), 128.4, 127.9, 127.75, 127.58, 114.4, 112.2 (d, J = 2.5 Hz), 110.2 (d, J = 21.0 Hz), 103.3 (d, J = 26.1 Hz), 69.2, 58.4, 55.1, 46.5. HRMS (ESI) m/z $[M + H]^+$ calcd for $C_{24}H_{23}FN_3O_3$, 420.1718; found, 420.1715.

General procedure for the synthesis of tripeptide Bz-Arg-Lys-4-Bn-O-Phg-β-lactam derivatives. Dipeptide Bz-Arg(Pbf)-Lys(Boc)-OH (1.0 equiv) and corresponding 4-Bn-O-Phg-β-lactam derivative (1.0 equiv) were dissolved in DMF (2 mL) and the solution was brought to pH 8 by addition of TMP (2.2 equiv). Temperature was decreased to 0 °C and COMU (1.1 equiv) was added. The reaction proceeded at 0 °C for 1 h and additional 3 h at room temperature. Ethyl acetate (30 mL) was added and the solution was washed with 1 M HCl (2 × 25 mL), saturated $NaHCO_3$ (2 × 25 mL) and saturated NaCl solution (2 × 25 mL). The organic layer was dried with $MgSO_4$ and evaporated to dryness. The crude protected product was redissolved in a 1:1 mixture of TFA and dichloromethane (2 mL). The solution was stirred at room temperature for 2 h and then brought to pH 12 by addition of 1 M NaOH. The product was extracted with ethyl acetate (2 × 30 mL). The combined organic layers were dried with $MgSO_4$ and evaporated to dryness. The crude product was purified by preparative HPLC.

Bz-Arg-Lys-4-Bn-O-Phg-(3*R*)-3-amino-1-phenylazetidin-2-one ((3*R*)-11a). Obtained as a white solid (10 mg, 41%) from (3*R*)-**10a** (12 mg, 30 μmol) and dipeptide Bz-Arg(Pbf)-Lys(Boc)-OH (23 mg, 30 μmol) with addition of COMU (14 mg, 33 μmol) and TMP (8.8 μL, 66 μmol). ^{1}H NMR (500 MHz, CD_3OD) δ 7.84 (d, J = 7.2 Hz, 2H), 7.57 (tt, J = 7.4, 2.0 Hz, 1H), 7.48 (t, J = 7.6 Hz, 2H), 7.43–7.42 (m, 2H), 7.38–7.30 (m, 9H), 7.13–7.09 (m, 1H), 7.01 (d, J = 8.7 Hz, 2H), 5.35 (s, 1H), 5.10 (s, 2H), 5.02 (dd, J = 5.6, 2.7 Hz, 1H), 4.53 (t, J = 7.1 Hz, 1H), 4.40 (dd, J = 9.1, 5.5 Hz, 1H), 3.99 (t, J = 5.7 Hz, 1H), 3.68 (dd, J = 5.7, 2.8 Hz, 1H), 3.14 (td, J = 6.9, 2.8 Hz, 2H), 2.88 (t, J = 7.6 Hz, 2H), 1.97–1.89 (m, 1H), 1.86–1.78 (m, 1H), 1.76–1.71 (m, 1H), 1.68–1.62 (m, 4H), 1.52–1.41 (m, 3H). ^{13}C NMR (126 MHz, CD_3OD) δ 174.5, 173.6, 173.1, 170.4, 166.0, 160.4, 158.5, 139.3, 138.5, 135.0, 133.1, 130.29, 130.26, 130.19, 129.6, 129.5, 129.0, 128.5, 128.5, 125.5, 117.8, 116.4, 71.0, 58.5, 56.7, 54.9, 54.5, 47.6, 42.1, 40.5, 31.8, 30.2, 28.0, 26.3, 23.7. HRMS (ESI) m/z $[M + H]^+$ calcd for $C_{43}H_{52}N_9O_6$, 790.4035; found, 790.4025.

Bz-Arg-Lys-4-Bn-O-Phg-(3*S*)-3-amino-1-phenylazetidin-2-one ((3*S*)-11a). Obtained as a yellow solid (11 mg, 14%) from (3*S*)-**10a** (38 mg, 95 μmol) and dipeptide Bz-Arg(Pbf)-Lys(Boc)-OH (72 mg, 95 μmol) with addition of COMU (45 mg, 104 μmol) and TMP (13.8 μL, 104 μmol). ^{1}H NMR (500 MHz, CD_3OD) δ 7.81 (d, J = 7.4 Hz, 2H), 7.55 (t, J = 7.4 Hz, 1H), 7.47–7.41 (m, 4H), 7.38–7.29 (m, 9H), 7.12 (t, J = 7.2 Hz, 1H), 7.01 (d, J = 8.6 Hz, 2H), 5.38 (s, 1H), 5.10 (s, 2H), 5.01 (dd, J = 5.5, 2.7 Hz, 1H), 4.55 (t, J = 7.1 Hz, 1H), 4.40 (dd, J = 9.0, 5.4 Hz, 1H), 3.98 (t, J = 5.6 Hz, 1H), 3.72 (dd, J = 5.7, 2.7 Hz, 1H), 3.20 (t, J = 7.0 Hz, 2H), 2.88 (t, J = 7.5 Hz, 2H), 2.00–1.93 (m, 1H), 1.89–1.80 (m, 2H), 1.76–1.58 (m, 5H), 1.53–1.38 (m, 2H). ^{13}C NMR (126 MHz, CD_3OD) δ 174.5, 173.5, 173.0, 170.4, 165.92, 160.4, 158.6, 139.3, 138.5, 135.0, 133.0, 130.37, 130.29, 130.21, 129.6, 129.5, 128.9, 128.5, 125.5, 117.8, 117.0, 116.4, 71.0, 58.3, 56.6, 54.9, 54.5, 47.5, 42.1, 40.5, 31.8, 30.2, 28.0, 26.3, 23.7. HRMS (ESI) m/z $[M + H]^+$ calcd for $C_{43}H_{52}N_9O_6$, 790.4035; found, 790.4018.

Bz-Arg-Lys-4-Bn-O-Phg-(3*R*)-3-amino-1-(4-methylphenyl) azetidin-2-one ((3*R*)-11b). Obtained as a yellow solid (19 mg, 36%) from (3*R*)-**10b** (27 mg, 65 μmol) and dipeptide Bz-Arg(Pbf)-Lys(Boc)-OH (49 mg, 65 μmol) with addition of COMU (31 mg, 72 μmol) and TMP (19.0 μL, 143 μmol). ^{1}H NMR (500 MHz, CD_3OD) δ 7.84 (d, J = 7.2 Hz, 2H), 7.57 (tt, J = 7.4, 1.1 Hz, 1H), 7.48 (t, J = 7.6 Hz, 2H), 7.42 (d, J = 7.3 Hz, 2H), 7.38–7.29 (m, 5H), 7.25 (d, J = 8.4 Hz, 2H), 7.13 (d, J = 8.2 Hz, 2H), 7.01 (d, J = 8.7 HZ, 2H), 5.34 (s, 1H), 5.10 (s, 2H), 5.02 (dd, J = 5.6, 2.7 Hz, 1H), 4.53 (t, J = 7.0 Hz, 1H), 4.39 (dd, J = 8.9, 5.7 Hz, 1H), 3.96 (t, J = 5.7 Hz, 1H), 3.64 (dd, J = 5.7, 2.7 Hz, 1H), 3.13 (td, J = 7.1, 5.0 Hz, 2H), 2.88 (t, J = 7.6 Hz, 2H), 2.29 (s, 3H), 1.96–1.89 (m, 1H), 1.85–1.61 (m, 7H), 1.53–1.38 (s, 2H). ^{13}C NMR (126 MHz, CD_3OD) δ 174.5, 173.6, 173.1, 170.3, 165.8, 160.4, 158.5, 138.5, 136.9, 135.5, 135.0, 133.1, 130.7, 130.27, 130.19, 129.6, 129.5, 128.9, 128.53, 128.50, 117.7, 116.4, 71.0, 58.5, 56.6, 54.9, 54.5, 47.7, 42.1, 40.5, 31.8, 30.3, 28.0, 26.3, 23.7, 20.9. HRMS (ESI) m/z $[M + H]^+$ calcd for $C_{44}H_{54}N_9O_6$, 804.4192; found, 804.4197.

Bz-Arg-Lys-4-Bn-O-Phg-(3*S*)-3-amino-1-(4-methylphenyl) azetidin-2-one ((3*S*)-11b). Obtained as a white solid (8 mg, 11%) from (3*S*)-**10b** (37 mg, 89 μmol) and dipeptide Bz-Arg(Pbf)-Lys(Boc)-OH (68 mg, 89 μmol) with addition of COMU (42 mg, 98 μmol) and TMP (25.9 μL, 196 μmol). ^{1}H NMR (500 MHz, CD_3OD) δ 7.80 (d, J = 7.4 Hz, 2H), 7.56 (t, J = 7.4 Hz, 1H), 7.47–7.41 (m, 4H), 7.39–7.24 (m, 7H), 7.15 (d, J = 8.2 Hz, 2H), 7.01 (d, J = 8.7 Hz, 2H), 5.38 (s, 1H), 5.10 (s, 2H), 5.01 (dd, J = 5.5, 2.6 Hz, 1H), 4.55 (t, J = 7.1 Hz, 1H), 4.40 (dd, J = 8.9, 5.5 Hz, 1H), 3.95 (t, J = 5.6 Hz, 1H), 3.70 (dd, J = 5.6, 2.7 Hz, 1H), 3.20 (t, J = 7.0 Hz, 2H), 2.88 (t, J = 7.5 Hz, 2H), 2.29 (s, 3H), 2.00–1.91 (m, 1H), 1.90–1.80 (m, 2H), 1.78–1.57 (m, 5H), 1.53–1.35 (m, 2H). ^{13}C NMR (126 MHz, CD_3OD) δ 174.5, 173.5, 173.0, 170.4, 165.7, 160.4, 158.6, 138.5, 136.9, 135.4, 135.0, 133.0, 130.7, 130.4, 130.2, 129.6, 129.5, 128.9, 128.51, 128.49, 117.8, 116.4, 71.0, 58.3, 56.6, 54.8, 54.5, 47.5, 42.1, 40.4, 31.8, 30.2, 28.0, 26.3, 23.7, 21.0. HRMS (ESI) m/z $[M + H]^+$ calcd for $C_{44}H_{54}N_9O_6$, 804.4192; found, 804.4172.

Bz-Arg-Lys-4-Bn-O-Phg-(3*R*)-3-amino-1-(3-methylphenyl) azetidin-2-one ((3*R*)-11c). Obtained as a white powder (14 mg, 40%) from (3*R*)-**10c** (18 mg, 43 μmol) and dipeptide Bz-Arg(Pbf)-Lys(Boc)-OH (33 mg, 43 μmol) with addition of COMU (20 mg, 47 μmol) and TMP (12.5 μL, 95 μmol). ^{1}H NMR (500 MHz, CD_3OD) δ 7.85 (d, J = 7.2 Hz, 2H), 7.56 (t, J = 7.4 Hz, 1H), 7.48 (t, J = 7.6 Hz, 2H), 7.44–7.40 (m, 2H), 7.38–7.29 (m,

5H), 7.23–7.09 (m, 3H), 7.01 (d, *J* = 8.7 Hz, 2H), 6.94 (d, *J* = 7.6 Hz, 1H), 5.34 (s, 1H), 5.11 (s, 2H), 5.01 (dd, *J* = 5.5, 2.6 Hz, 1H), 4.53 (dd, *J* = 7.3, 6.7 Hz, 1H), 4.38 (dd, *J* = 8.9, 5.7 Hz, 1H), 3.97 (t, *J* = 5.7 Hz, 1H), 3.66 (dd, *J* = 5.7, 2.7 Hz, 1H), 3.17–3.07 (m, 2H), 2.88 (t, *J* = 7.5 Hz, 2H), 2.29 (s, 3H), 1.96–1.61 (m, 8H), 1.54–1.38 (m, 2H). ^{13}C NMR (126 MHz, CD_3OD) δ 174.5, 173.6, 173.1, 170.3, 166.0, 160.4, 158.5, 140.5, 139.3, 138.5, 134.9, 133.1, 130.3, 130.17, 130.15, 129.63, 129.53, 128.9, 128.55, 128.50, 126.3, 118.3, 116.4, 114.9, 71.0, 58.5, 56.6, 54.9, 54.6, 47.7, 42.0, 40.5, 31.7, 30.3, 28.0, 26.3, 23.7, 21.5. HRMS (ESI) *m/z* $[M + H]^+$ calcd for $C_{44}H_{54}N_9O_6$, 804.4192; found, 804.4190.

Bz-Arg-Lys-4-Bn-O-Phg-(3*S*)-3-amino-1-(3-methylphenyl) azetidin-2-one ((3*S*)-11c). Obtained as a white powder (14 mg, 30%) from (3*S*)-**10c** (25 mg, 59 μmol) and dipeptide Bz-Arg(Pbf)-Lys(Boc)-OH (45 mg, 59 μmol) with addition of COMU (28 mg, 65 μmol) and TMP (17.2 μL, 130 μmol). ^{1}H NMR (500 MHz, CD_3OD) δ 7.81 (d, *J* = 7.3 Hz, 2H), 7.56 (t, *J* = 7.4 Hz, 1H), 7.47–7.71 (m, 4H), 7.39–7.29 (m, 5H), 7.24–7.21 (m, 2H), 7.17 (d, *J* = 8.3 Hz, 1H), 7.02 (d, *J* = 8.7 Hz, 2H), 6.97–6.95 (m, 1H), 5.39 (s, 1H), 5.11 (s, 2H), 5.00 (dd, *J* = 5.6, 2.7 Hz, 1H), 4.55 (dd, *J* = 7.4, 6.8 Hz, 1H), 4.41 (dd, *J* = 9.1, 5.5 Hz, 1H), 3.96 (t, *J* = 5.6 Hz, 1H), 3.71 (dd, *J* = 5.7, 2.8 Hz, 1H), 3.21 (t, *J* = 7.0 Hz, 2H), 2.88 (t, *J* = 7.5 Hz, 2H), 2.32 (s, 3H), 2.01–1.93 (m, 1H), 1.90–1.81 (m, 2H), 1.77–1.61 (m, 5H), 1.53–1.39 (m, 2H). ^{13}C NMR (126 MHz, CD_3OD) δ 174.5, 173.5, 173.0, 170.4, 165.9, 160.4, 158.6, 140.5, 139.3, 138.5, 135.0, 133.0, 130.4, 130.20, 130.16, 129.62, 129.53, 128.9, 128.51, 128.50, 126.3, 118.3, 116.4, 115.0, 71.0, 58.3, 56.5, 54.9, 54.5, 47.5, 42.1, 40.5, 31.8, 30.2, 28.0, 26.4, 23.7, 21.5. HRMS (ESI) *m/z* $[M + H]^+$ calcd for $C_{44}H_{54}N_9O_6$, 804.4192; found, 804.4199.

Bz-Arg-Lys-4-Bn-O-Phg-(3*R*)-3-amino-1-(4-fluorophenyl) azetidin-2-one ((3*R*)-11d). Obtained as a white solid (10 mg, 42%) from (3*R*)-**10d** (13 mg, 31 μmol) and dipeptide Bz-Arg(Pbf)-Lys(Boc)-OH (24 mg, 31 μmol) with addition of COMU (15 mg, 34 μmol) and TMP (15.8 μL, 119 μmol, 3.5 equiv). ^{1}H NMR (500 MHz, CD_3OD) Major isomer δ 7.86–7.82 (m, 2H), 7.59–7.54 (m, 1H), 7.48 (t, *J* = 7.6 Hz, 2H), 7.44–7.29 (m, 8H), 7.13–7.06 (m, 3H), 7.01 (d, *J* = 8.1 Hz, 2H), 5.35 (s, 1H), 5.10 (s, 2H), 5.02 (dd, *J* = 5.6, 2.7 Hz, 1H), 4.53 (t, *J* = 7.1 Hz, 1H), 4.40 (dd, *J* = 8.5, 6.0 Hz, 1H), 3.98 (t, *J* = 5.6 Hz, 1H), 3.67 (dd, *J* = 5.7, 2.7 Hz, 1H), 3.16 (td, *J* = 7.1, 2.3 Hz, 2H), 2.88 (t, *J* = 7.5 Hz, 2H), 1.98–1.90 (m, 1H), 1.88–1.78 (m, 2H), 1.76–1.59 (m, 5H), 1.53–1.40 (m, 2H); minor isomer δ 7.86–7.82 (m, 2H), 7.59–7.54 (m, 1H), 7.48 (t, *J* = 7.6 Hz, 2H), 7.44–7.29 (m, 8H), 7.13–7.06 (m, 3H), 7.01 (d, *J* = 8.1 Hz, 2H), 5.14 (s, 2H), 5.04 (m, 1H), 4.95 (s, 1H), 4.53 (t, *J* = 7.1 Hz, 1H), 4.40 (dd, *J* = 8.5, 6.0 Hz, 1H), 3.98 (t, *J* = 5.6 Hz, 1H), 3.64–3.62 (m, 1H), 3.16 (td, *J* = 7.1, 2.3 Hz, 2H), 2.88 (t, *J* = 7.5 Hz, 2H), 1.98–1.90 (m, 1H), 1.88–1.78 (m, 2H), 1.76–1.59 (m, 5H), 1.53–1.40 (m, 2H). ^{13}C NMR (126 MHz, CD_3OD) both isomers δ 174.5, 173.6, 173.1, 170.4, 169.5, 165.8, 165.3, 161.75, 161.72, 161.56, 160.45, 160.42, 159.8, 158.6, 138.5, 138.2, 135.8 (d, *J* = 2.7 Hz), 135.0, 133.08, 132.97, 131.0, 130.26, 130.19, 129.64, 129.60, 129.56, 129.54, 129.03, 128.95, 128.55, 128.53, 128.50, 128.39, 126.1, 119.42 (d, *J* = 8.0 Hz), 119.39 (d, *J* = 8.0 Hz),, 116.98 (d, *J* = 23.1 Hz), 116.95, 116.80 (d, *J* = 23.1 Hz), 116.4, 71.05, 71.01, 58.4, 57.5, 56.89, 56.77, 54.9, 54.4, 52.6, 47.81, 47.68, 42.4, 42.1, 40.5, 31.9, 30.2, 28.0, 26.3, 23.7. HRMS (ESI) *m/z* $[M + H]^+$ calcd for $C_{43}H_{50}FN_9O_6$, 808.3941; found, 808.3937.

Bz-Arg-Lys-4-Bn-O-Phg-(3*S*)-3-amino-1-(4-fluorophenyl) azetidin-2-one ((3*S*)-11d). Obtained as a white solid (15 mg, 57%) from (3*S*)-**10d** (14 mg, 34 μmol) and dipeptide Bz-Arg(Pbf)-Lys(Boc)-OH (26 mg, 34 μmol) with addition of COMU (16 mg, 37 μmol) and TMP (9.9 μL, 75 μmol). ^{1}H NMR (500 MHz, CD_3OD) δ 7.82 (d, *J* = 7.3 Hz, 2H), 7.56 (t, *J* = 7.4 Hz, 1H), 7.50–7.27 (m, 11H), 7.13–7.05 (m, 2H), 7.01 (d, *J* = 8.7 Hz, 2H), 5.38 (s, 1H), 5.10 (s, 2H), 5.00 (dd, *J* = 5.5, 2.7 Hz, 1H), 4.55 (t, *J* = 7.0 Hz, 1H), 4.41 (dd, *J* = 9.0, 5.5 Hz, 1H), 3.96 (t, *J* = 5.7 Hz, 1H), 3.71 (dd, *J* = 5.6, 2.7 Hz, 1H), 3.21 (t, *J* = 7.0 Hz, 2H), 2.88 (t, *J* = 7.5 Hz, 2H), 2.01–1.92 (m, 1H), 1.91–1.80 (m, 2H), 1.78–1.56 (m, 5H), 1.55–1.36 (m, 2H). ^{13}C NMR (126 MHz, CD_3OD) δ 174.5, 173.5, 173.0, 170.4, 165.7, 161.7 (d, *J* = 243.5 Hz), 160.4, 158.6, 138.5, 135.8 (d, *J* = 2.4 Hz), 135.03, 133.0, 131.0, 130.4, 130.2, 129.61, 129.53, 128.9, 128.51, 128.50, 119.4 (d, *J* = 8.0 Hz),, 116.9 (d, *J* = 23.0 Hz), 116.36, 71.00, 58.3, 56.9, 55.0, 54.5, 47.7, 42.1, 40.5, 31.9, 30.2, 28.0, 26.4, 23.6. HRMS (ESI) *m/z* $[M + H]^+$ calcd for $C_{43}H_{51}FN_9O_6$, 808.3941; found, 808.3922.

Bz-Arg-Lys-4-Bn-O-Phg-(3*R*)-3-amino-1-(3-fluorophenyl) azetidin-2-one ((3*R*)-11e). Obtained as a white solid (5 mg, 22%) from (3*R*)-**10e** (13 mg, 31 μmol) and dipeptide Bz-Arg(Pbf)-Lys(Boc)-OH (24 mg, 31 μmol) with addition of COMU (15 mg, 34 μmol) and TMP (9.0 μL, 68 μmol). ^{1}H NMR (500 MHz, CD_3OD) major isomer δ 7.87–7.82 (m, 2H), 7.56 (t, *J* = 7.4 Hz, 1H), 7.48 (t, *J* = 7.6 Hz, 2H), 7.44–7.41 (m, 2H), 7.39–7.28 (m, 5H), 7.23–7.19 (m, 1H), 7.15–7.08 (m, 2H), 7.01 (d, *J* = 8.8 Hz, 2H), 6.89–6.83 (m, 1H), 5.35 (s, 1H), 5.10 (s, 2H), 5.02 (dd, *J* = 5.7, 3.0, Hz, 1H), 4.53 (t, *J* = 7.1 Hz, 1H), 4.41 (dd, *J* = 9.2, 5.5 Hz, 1H), 4.00 (t, *J* = 5.7 Hz, 1H), 3.70 (dd, *J* = 5.8, 2.9 Hz, 1H), 3.16 (td, *J* = 7.1, 1.8 Hz, 2H), 2.88 (t, *J* = 7.6 Hz, 2H), 1.98–1.89 (m, 1H), 1.88–1.79 (m, 2H), 1.77–1.59 (m, 5H), 1.56–1.36 (m, 2H). minor isomer δ 7.87–7.82 (m, 2H), 7.56 (t, *J* = 7.4 Hz, 1H), 7.48 (t, *J* = 7.6 Hz, 2H), 7.44–7.41 (m, 2H), 7.39–7.28 (m, 5H), 7.23–7.19 (m, 1H), 7.15–7.08 (m, 2H), 7.01 (d, *J* = 8.8 Hz, 2H), 6.89–6.83 (m, 1H), 5.14 (s, 2H), 5.04 (dd, *J* = 5.8, 2.8 Hz, 1H), 4.96 (s, 1H), 4.53 (t, *J* = 7.1 Hz, 1H), 4.41 (dd, *J* = 9.2, 5.5 Hz, 1H), 4.00 (t, *J* = 5.7 Hz, 1H), 3.66 (dd, *J* = 5.8, 2.9 Hz, 1H), 3.16 (td, *J* = 7.1, 1.8 Hz, 2H), 2.88 (t, *J* = 7.6 Hz, 2H), 1.98–1.89 (m, 1H), 1.88–1.79 (m, 2H), 1.77–1.59 (m, 5H), 1.56–1.36 (m, 2H). ^{13}C NMR (126 MHz, CD_3OD) both isomers δ 174.5, 173.6, 173.1, 170.4, 166.3, 165.8, 164.5 (d, *J* = 244.5 Hz), 161.6, 160.4, 158.5, 140.8 (d, *J* = 11.9 Hz), 138.5, 138.2, 135.0, 133.1, 131.99 (d, *J* = 9.3 Hz), 131.95 (d, *J* = 9.6 Hz), 131.0, 130.26, 130.15, 129.63, 129.56, 129.54, 129.03, 128.95, 128.56, 128.52, 128.51, 126.0, 117.0, 116.4, 113.34 (d, *J* = 3.2 Hz), 113.31 (d, *J* = 3.3 Hz), 111.97 (d, *J* = 21.7 Hz), 111.96 (d, *J* = 21.4 Hz), 105.2 (d, *J* = 26.0 Hz), 71.05, 71.01, 58.4, 57.5, 56.9, 56.8, 55.0, 54.4, 47.8, 47.7, 42.1, 40.5, 31.9, 30.2, 28.0, 26.3, 23.7. HRMS (ESI) *m/z* $[M + H]^+$ calcd for $C_{43}H_{51}FN_9O_6$, 808.3941; found, 808.3931.

Bz-Arg-Lys-4-Bn-O-Phg-(3*S*)-3-amino-1-(3-fluorophenyl) azetidin-2-one ((3*S*)-11e). Obtained as a white solid (11 mg, 35%) from (3*S*)-**10e** (16 mg, 37 μmol) and dipeptide Bz-Arg(Pbf)-Lys(Boc)-OH (28 mg, 37 μmol) with addition of COMU (17 mg, 41 μmol) and TMP (10.8 μL, 81 μmol). ^{1}H NMR (500 MHz, CD_3OD) δ 7.83–7.80 (m, 2H), 7.54 (tt, *J* = 7.4, 1.2 Hz, 1H), 7.49–7.39 (m, 4H), 7.39–7.27 (m, 6H), 7.21 (dt, *J* = 10.3, 2.2 Hz, 1H),

7.14–7.07 (m, 1H), 7.00 (d, J = 8.8 Hz, 2H), 6.85 (td, J = 8.5, 2.5 Hz, 1H), 5.37 (s, 1H), 5.09 (s, 2H), 4.99 (dd, J = 5.7, 2.9 Hz, 1H), 4.54 (dd, J = 7.6, 6.6 Hz, 1H), 4.41 (dd, J = 9.1, 5.5 Hz, 1H), 3.97 (t, J = 5.8 Hz, 1H), 3.71 (dd, J = 5.8, 2.9 Hz, 1H), 3.21 (t, J = 7.0 Hz, 2H), 2.87 (t, J = 7.6 Hz, 2H), 2.00–1.91 (m, 1H), 1.90–1.79 (m, 2H), 1.76–1.56 (m, 5H), 1.53–1.37 (m, 2H). ^{13}C NMR (126 MHz, CD_3OD) δ 174.5, 173.5, 173.0, 170.4, 166.2, 164.5 (d, J = 244.5 Hz), 160.4, 158.6, 140.8 (d, J = 10.8 Hz), 138.5, 135.0, 133.0, 132.0 (d, J = 9.4 Hz), 130.33, 130.20, 129.61, 129.53, 128.9, 128.51, 128.50, 116.4, 113.3 (d, J = 2.9 Hz), 112.0 (d, J = 21.6 Hz), 105.2 (d, J = 25.9 Hz), 71.0, 58.3, 56.9, 55.0, 54.4, 47.7, 42.1, 40.5, 31.9, 30.1, 28.0, 26.4, 23.6. HRMS (ESI) m/z $[M + H]^+$ calcd for $C_{43}H_{51}FN_9O_6$, 808.3941; found, 808.3924.

Fluorimetric DENV and WNV protease assay. The assays were performed as previously described.[43] Briefly, the measurements were performed in black 96 well V-bottom plates (Greiner Bio-One, Germany) using excitation and emission wavelengths of 320 and 405 nm, respectively. In the initial screening, the inhibitors were tested in 50 μM final concentration (from 10 mM DMSO Stock solution). The compounds were preincubated with the DENV (final concentration 100 nM) or WNV (final concentration 150 nM) protease in the assay buffer (50 mM Tris-HCl pH 9, ethylene glycol (10% v/v), and 0.0016% Brij 58) for 15 minutes, after which the corresponding FRET substrate (final concentration 50 μM) was added, making a final assay volume 100 μL per well. The reaction was monitored continuously for 15 minutes and the enzymatic activity was determined as slope per second (RFU/s). Percentage inhibition was calculated relative to a control without inhibitor. IC_{50} values were determined in compounds that showed > 70% inhibition at 50 μM concentration. The activity at 7 different concentrations of an inhibitor was measured using the same protocol and IC_{50} value was calculated from the curve obtained with a nonlinear fit of dose response using equation for [inhibitor] vs. normalized response with variable slope in GraphPad Prism 6 software (GraphPad Software, Inc., USA). All measurements were performed in triplicates and the results are expressed as an average value.

Tryptophan quenching assay. The samples were prepared and measured in black 96 well V-bottom plates (Greiner Bio-One, Germany) using 280 nm as an excitation and 340 nm as an emission wavelength. DENV protease in concentration 200 nM was used in all measurements and samples were prepared in assay buffer (50 mM Tris-HCl pH 9, ethylene glycol (10% v/v), and 0.0016% Brij 58). For the determination of competitive binding, compound (3*S*)-**11a** in final concentrations 20 μM and 60 μM was added to the protease. The addition of the quencher **MB-211** in the concentration range 0–20 μM followed immediately. The final volume was 100 μL per well. The fluorescence was measured 5 minutes after the addition of the quencher. For the evaluation of reversible binding, inhibitor (3*S*)-**11a** in concentration 60 μM was preincubated for 16 h with the protease before the addition of the quencher (0–20 μM). The fluorescence was measured 5 minutes after the addition of quencher. As a control, a sample without inhibitor preincubation was used. The role of the Ser135 was evaluated as described for the competitive binding, using the S135A mutant protease instead of the active form. The fluorescence quenching in the active protease served as a control. The inner filter effect (IFE) was evaluated using *N*-acetyltryptophanamide (NATA) in the concentration 1 μM instead of the protease in combination with MB-211 in the concentration range 0 – 20 μM. All measurements were performed in triplicates and expressed as an average value. The results are presented as fluorescence intensity relative to the fluorescence without the addition of the quencher.

Dilution experiment. The fluorimetric assay was performed in black 96 well V-bottom plates (Greiner Bio-One, Germany) using excitation and emission wavelengths of 320 and 405 nm, respectively. The inhibitor in high concentration (60 μM, 20 × IC_{50}) and low concentration (1.7 μM, 0.5 × IC_{50}) was preincubated with DENV protease (3 μM) in the assay buffer (50 mM Tris-HCl pH 9, ethylene glycol (10% v/v), and 0.0016% Brij 58) for 3 h or 6 h. The control without inhibitor (equal volume of DMSO) was incubated with the protease accordingly. The preincubated inhibitor and control solutions were pipetted into a 96 well plate together with the assay buffer and additional amount of inhibitor to prepare the final diluted inhibitor solution (1.7 μM) and control solutions: 20 × IC_{50} concentration control (60 μM,); 0.5 × IC_{50} inhibitor controls (1.7 μM) and control without inhibitor. The diluted inhibitor solution was prepared by mixing the high concentration preincubated solution (3.33 μL) and assay buffer (86.66 μL). The 20 × IC_{50} control was prepared by the addition of the same preincubated solution (3.33 μL), assay buffer (38.35 μL) and inhibitor (48.35 μL from 200 μM solution prepared from the 10 mM Stock solution). The 0.5 × IC_{50} control was prepared from low concentration preincubated solution (3.33 μL), assay buffer (38.35 μL) and inhibitor (48.35 μL from 6.66 μM solution prepared from the 10 mM Stock solution), whereas the control without inhibitor was prepared from the preincubated DMSO control (3.33 μL) and assay buffer (86.66 μL). Additional 0.5 × IC_{50} inhibitor control without preincubation was used in the experiment with 6 h preincubation. This control was prepared analogously to preincubated 0.5 × IC_{50} inhibitor control, but immediately before the measurement. The protease concentration was 100 nM in each final solution. The enzymatic reaction was initiated by the addition of the FRET substrate (10 μL, final concentration 50 μM) at 0, 30, 60 and 120 minutes after the end of the preincubation. The reaction was monitored continuously for 15 minutes and the enzymatic activity was determined as slope per second (RFU/s). Percentage inhibition was calculated relative to the control without inhibitor. The measurements were performed in triplicates and the results are expressed as an average value.

LC-MS measurement. Compounds (3*S*)-**11a** and **MB-53** in concentration 100 μM were incubated with either active DENV protease or inactive S135A mutant protease (final concentration in both cases 3 μM) or in the assay buffer without the addition of the protease (50 mM Tris-HCl pH 9, ethylene glycol (10% v/v), and 0.0016% Brij 58). Each hour in the 11 h period, a volume of 15 μL of incubated solution was subjected to LC-MS analysis. The measurements were performed on an Agilent 1200 series HPLC device in combination with ESI-MS micrOTOF-QII instrument (Bruker Daltonik, Germany) using Reprosil-Pur ODS-3, Dr. Maisch GmbH, Germany, 3 μm, 50 x 2 mm HPLC column. Used method was as follows: eluent A - water (0.1% formic acid), eluent B - acetonitrile (0.1% formic acid): 0 min – 4.0 min gradient 10% B – 95% B, 4.1 min – 8.0 min isocratic 95% B, 8.1 min – 19.0 min isocratic 10% B; flow rate 0.3 mL/min. MS measurements were per-

formed in negative mode with external mass calibration and Na-formate as a calibration standard.

Docking studies. Autodock Vina 1.1.2[44] was used for docking studies of tripeptide-β-lactam (3*S*)-**11a**. 3D structures of the compounds were built using Maestro software. Protein structures were prepared for docking calculations starting from the crystal structure of DENV serotype 3 NS2B-NS3 protease in complex with tetrapeptidyl aldehyde (PDB code: 3U1I). Only protein atoms were kept for the docking calculations, while water molecules and other molecules present in the crystal structures were removed. Docking preparation was performed with Autodock Tools[45] using default settings. The grid size was adjusted to the size of the ligand and the size of the active site (74 Å × 78 Å × 64 Å). The grid spacing was 1.0. The results were analyzed with Autodock Vina and Maestro. Visualization was performed with UCSF Chimera.[46]

Cell culture. Huh-7 and Vero E6 cells were maintained in DMEM supplemented with 100 U/mL penicillin, 100 µg/mL of streptomycin, and 10% heat-inactivated FCS. During infection of Huh-7 cells, DMEM was supplemented with 10 mM HEPES.

Virus titer reduction assay. Huh-7 cells were seeded into 96-well plates at a density of 1×10^4 cells per well and incubated overnight. The next day, cells were infected with DENV serotype 2 for 2 h at an MOI of 1, before medium change and compound addition. Infected cells were then incubated for 48 h in the presence of compound in triplicate wells. In order to determine the EC_{50}, a range of serial diluted compound concentrations starting at 50 µM was used. After 48 h incubation, supernatants were harvested and triplicates pooled. These virus containing supernatants were used to determine the virus titer (reduction) by plaque assay, as described elsewhere.[47]

Briefly, VeroE6 cells were seeded into 24-well plates at a density of 2.5×10^5 cells/well and the next day infected for 1 h with 10 fold serial dilutions of virus supernatant ranging from 10^{-1} to 10^{-6}. After medium exchange and addition of the plaque medium VeroE6 cells were incubated for 7 days. Cells were subsequently fixed with formaldehyde and plaques visualized by crystal violet stain.

At a suitable dilution, plaques were counted, the virus titer calculated and plotted against the respective compound concentration. EC_{50} values were calculated from the curves obtained with a non-linear fit of dose response using equation for [inhibitor] vs. normalized response with variable slope in GraphPad Prism 6 software (GraphPad Software, Inc., USA).

Cytotoxicity. Cell viability in presence of compound dilutions was determined in parallel to the virus titer reduction assay using CellTiter-Blue® (Promega) according to the manufacturer's instructions.

ASSOCIATED CONTENT

Synthetic procedures for β-lactams (3*R*)- and (3*S*)-**3a–e**, synthetic procedures for dipeptides, yields of dipeptide-β-lactam derivatives, ratio of epimers of tripeptide-β-lactam derivatives, inhibitor dose-response curves in biochemical and cell assays, off-target activity against thrombin and trypsin, expression and purification of DENV proteases, the structure and binding analysis of **MB-211**, MS spectra of (3*S*)-**11a** and its cleavage products after incubation with DENV protease, cleavage of **MB-53** by DENV protease, docking additional conformations and H-bonds, NMR spectra and HPLC chromatograms of final di- and tripeptide-β-lactam derivatives, molecular formula strings. This material is available free of charge via the Internet at http://pubs.acs.org.

AUTHOR INFORMATION

Corresponding Author

* E-mail: tdrazic@uni-heidelberg.de. Phone: +49 (0)6221 – 54 4820. Fax: +49-6221-546430.

Present Addresses

[§]ICIQ-Institute of Chemical Research of Catalonia, Avenida Països Catalans 16, 43007 Tarragona, Spain

[‡]UCL School of Pharmacy, 29-39 Brunswick Square, Bloomsbury, London, WC1N 1AX, UK

Author Contributions

All authors have given approval to the final version of the manuscript.

Notes

The authors declare no competing financial interest.

ACKNOWLEDGMENT

We thank Marija Spiric for the synthesis of precursors, Luuk van Oosten for the help in expression and purification of the DENV protease, Dr. Mira A. M. Behnam for providing compounds MB-53 and MB-211, Stefan Hinkes for discussions and critically reading the manuscript, Tobias Timmermann for NMR measurements, Heiko Rudy for measuring ESI-MS spectra and Natascha Stefan for performing biochemical assays. Tonko Dražić gratefully acknowledges financial support from the European Union's Horizon 2020 research and innovation program under the Marie Skłodowska-Curie grant agreement No 748447 (LIsTEN).

ABBREVIATIONS

COMU, (1-cyano-2-ethoxy-2-oxoethylidenaminooxy)-dimethylamino-morpholino-carbenium hexafluorophosphate; CTC, 2-chlorotrytil chloride; DMEM, Dulbecco's modified Eagle medium; FCS, fetal calf serum; HEPES, 4-(2-hydroxyethyl)-1-piperazineethanesulfonic acid; IBCF, isobutyl chloroformate; NMM, *N*-methylmorpholine; SPPS, solid phase peptide synthesis; TMP, 2,4,6-trimethylpyridine.

REFERENCES

(1) Singh, J.; Petter, R. C.; Baillie, T. A.; Whitty, A. The resurgence of covalent drugs. *Nature Rev. Drug Discov.* **2011**, *10*, 307–317.

(2) Li, D.; Ambrogio, L.; Shimamura, T.; Kubo, S.; Takahashi, M.; Chirieac, L. R.; Padera, R. F.; Shapiro, G. I.; Baum, A.; Himmelsbach, F.; Rettig, W. J.; Meyerson, M.; Solca, F.; Greulich, H.; Wong, K. K. BIBW2992, an irreversible EGFR/HER2 inhibitor highly effective in preclinical lung cancer models. *Oncogene* **2008**, *27*, 4702–4711.

(3) Tsou, H. R.; Overbeek-Klumpers, E. G.; Hallett, W. A.; Reich, M. F.; Floyd, M. B.; Johnson, B. D.; Michalak, R. S.; Nilakantan, R.; Discafani, C.; Golas, J.; Rabindran, S. K.; Shen, R.; Shi, X.; Wang, Y. F.; Upeslacis, J.; Wissner, A. Optimization of 6,7-disubstituted-4-(arylamino)quinoline-3-carbonitriles as orally active, irreversible inhibitors of human epidermal growth factor receptor-2 kinase activity. *J. Med. Chem.* **2005**, *48*, 1107–1131.

(4) Paramore, A.; Frantz, S. Bortezomib *Nature Rev. Drug Discov.* **2003**, *2*, 611–612.

(5) de Leuw, P.; Stephan, C. Protease inhibitors for the treatment of hepatitis C virus infection. *GMS Infect. Dis.* **2017**, *5*, Doc08

(6) Bauer, R. A. Covalent inhibitors in drug discovery: From accidental discoveries to avoided liabilities and designed therapies. *Drug Discov. Today* **2015**, *20*, 1061–1073.

(7) Bhatt, S.; Gething, P. W.; Brady, O. J.; Messina, J. P.; Farlow, A. W.; Moyes, C. L.; Drake, J. M.; Brownstein, J. S.; Hoen, A. G.; Sankoh, O.; Myers, M. F.; George, D. B.; Jaenisch, T.; Wint, G. R. W.; Simmons, C. P.; Scott, T. W.; Farrar, J. J.; Hay, S. I. The global distribution and burden of dengue. *Nature* **2013**, *496*, 504–507.

(8) Bouzid, M.; Colón-González, F. J.; Tobias Lung, T.; Lake, I. R.; Hunter, P. R. Climate change and the emergence of vector-borne diseases in Europe: case study of dengue fever. *BMC Public Health* **2014**, *14*, 781.

(9) Colón-González, F. J.; Fezzi, C.; Lake, I. R.; Hunter, P. R. The effects of weather and climate change on dengue. *PLoS Negl. Trop. Dis.* **2013**, *7*, e2503.

(10) Nitsche, C.; Holloway, S.; Schirmeister, T.; Klein, C.D. Biochemistry and medicinal chemistry of the dengue virus protease. *Chem. Rev.* **2014**, *114*, 11348–11381.

(11) Boldescu, V.; Behnam, M. A. M.; Vasilakis, N.; Klein, C. D. Broad-spectrum agents for flaviviral infections: dengue, Zika and beyond. *Nature Rev. Drug Develop.* **2017**, *16*, 565–586.

(12) Yin, Z.; Patel, S. J.; Wang, W.-L.; Wang, G.; Chan, W.-L.; Rao, K. R. R.; Alam, J.; Jeyaraj, D. A.; Ngew, X.; Patel, V.; Beer, D.; Lim, S. P.; Vasudevan, S. G.; Keller, T. H. Peptide inhibitors of dengue virus NS3 protease. Part 1: Warhead. *Bioorg. Med. Chem. Lett.* **2006**, *16*, 36–39.

(13) Yin, Z.; Patel, S. J.; Wang, W. L.; Chan, W. L.; Ranga Rao, K. R.; Wang, G.; Ngew, X.; Patel, V.; Beer, D.; Knox, J. E.; Ma, N. L.; Ehrhardt, C.; Lim, S. P.; Vasudevan, S. G.; Keller, T. H. Peptide inhibitors of dengue virus NS3 protease. Part 2: SAR study of tetrapeptide aldehyde inhibitors. *Bioorg. Med. Chem. Lett.* **2006**, *16*, 40–43.

(14) Nitsche, C.; Zhang, L.; Weigel, L. F.; Schilz, J.; Graf, D.; Bartenschlager, R.; Hilgenfeld, R.; Klein, C. D. Peptide–boronic acid inhibitors of flaviviral proteases: Medicinal chemistry and structural biology. *J. Med. Chem.* **2017**, *60*, 511–516.

(15) Fiasella, A.; Nuzzi, A.; Summa, M.; Armirotti, A.; Tarozzo, G.; Tarzia, G.; Mor, M.; Bertozzi, F.; Bandiera, T.; Piomelli, D. 3-Aminoazetidin-2-one derivatives as *N*-acylethanolamine acid amidase (NAAA) inhibitors suitable for systemic administration. *ChemMedChem* **2014**, *9*, 1602–1614.

(16) Nuzzi, A.; Fiasella, A.; Ortega, J. A.; Pagliuca, C.; Ponzano, S.; Pizzirani, D.; Bertozzi, S. M.; Ottonello, G.; Tarozzo, G.; Reggiani, A.; Bandiera, T.; Bertozzi, F.; Piomelli, D. Potent α-amino-β-lactam carbamic acid ester as NAAA inhibitors. Synthesis and structure-activity relationship (SAR) studies. *Eur. J. Med. Chem.* **2016**, *111*, 138–159.

(17) Petracca, R.; Ponzano, S.; Bertozzi, S. M.; Sasso, O.; Piomelli, D. Bandiera, T.; Bertozzi, F. Progress in the development of β -lactams as *N*-acylethanolamine acid amidase (NAAA) inhibitors: Synthesis and SAR study of new, potent N-O-substituted derivatives. *Eur. J. Med. Chem.* **2017**, *126*, 561–575.

(18) Han, W. T.; Trehan, A. K.; Wright, J. J. K.; Federici, M. E.; Seiler, S. M.; Meanwell, N, A. Azetidin-2-one derivatives as inhibitors of thrombin. *Bioorg. Med. Chem.* **1995**, *3*, 1123–1143.

(19) Finke, P. E.; Shah, S. K.; Fletcher, D. S.; Ashe, B. M.; Brause, K. A.; Chandler, G. O.; Dellea, P. S.; Hand, K. M.; Maycock, A. L.; Osinga, D. G.; Underwood, D. J.; Weston, H.; Davies, P.; Doherty, J. B. Orally active β-lactam inhibitors of human leukocyte elastase. 3.[1] Stereospecific synthesis and structure-activity relationships for 3,3-dialkylazetidin-2-ones. *J. Med. Chem.* **1995**, *38*, 2449–2462.

(20) Ribeiro, A.; Pontis, S.; Mengatto, L.; Armirotti, A.; Chiurchiù, V.; Capurro, V.; Fiasella, A.; Nuzzi, A.; Romeo, E.; Moreno-Sanz, G.; Maccarrone, M.; Reggiani, A.; Tarzia, G.; Mor, M.; Bertozzi, F.; Bandiera, T.; Piomelli, D. A potent systemically active *N*-acylethanolamine acid amidase inhibitor that suppresses inflammation and human macrophage activation. *ACS Chem. Biol.* **2015**, *10*, 1838–1846.

(21) Vergely, I.; Boggetto, N.; Okochi, V.; Golpayegani, S.; Reboud-Ravaux, M.; Kobaiter, R.; Joyeau, R.; Wakselman M. Inhibition of human leukocyte elastase by functionalized *N*-aryl azetidin-2-ones: Substituent effects at C-3 and benzylic positions. *Eur. J. Med. Chem.* **1995**, *30*, 199–208.

(22) Hanessian, S.; Couture, C.; Wyss, H. Design and reactivity of organic functional groups-utility of imidazolylsulfonates in the synthesis of monobactams and 3-amino nocardicinic acid. *Can. J. Chem.* **1985**, *63*, 3613–3617.

(23) Behnam, M. A. M.; Graf, D.; Bartenschlager, R.; Zlotos, D. P.; Klein, C. D. Discovery of nanomolar dengue and West Nile virus protease inhibitors containing a 4-benzyloxyphenylglycine residue. *J. Med. Chem.* **2015**, *58*, 9354–9370.

(24) Vaughan, J. R. Acylalkylcarbonates as acylating agents for the synthesis of peptides *J. Am. Chem. Soc.* **1951**, *73*, 3547–3548.

(25) El-Faham, A.; Albericio, F. COMU: A third generation of uronium-type coupling reagents. *J. Pept. Sci.* **2010**, *16*, 6–9.

(26) Liang, C.; Behnam, M. A. M.; Sundermann, T. R.; Klein C. D. Phenylglycine racemization in Fmoc-based solid-phase peptide synthesis: Stereochemical stability is achieved by choice of reaction conditions. *Tetrahedron Lett.* **2017**, *58*, 2325–2329.

(27) Nitsche, C.; Behnam, M. A. M..; Steuer, C. Klein, C. D. Retro peptide-hybrids as selective inhibitors of the dengue virus NS2B-NS3 protease. *Anitviral Res.* **2012**, *94*, 72–79.

(28) Schüller, A., Yin, Z., Brian Chia, C.S., Doan, D. N. P., Kim, H.-K., Shang, L., Loh, T. P., Hill, J., Vasudevan, S. G.,. Tripeptide inhibitors of dengue and West Nile virus NS2B–NS3 protease. *Antiviral Res.* **2011**, *92*, 96–101.

(29) Behnam, M. A. M.; Nitsche, C.; Vechi, S. M.; Klein, C. D. C-Terminal residue optimization and fragment merging: Discovery of a potent peptide-hybrid inhibitor of dengue protease. *ACS Med. Chem. Lett.* **2014**, *5*, 1037–1042.

(30) Bodenreider, C.; Beer, D.; Keller, T. H.; Sonntag, S.; Wen, D.; Yap, L.; Yau, Y. H.; Shochat, S. G.; Huang, D.; Zhou, T.; Caflisch, A.; Su, X.-C.; Ozawa, K.; Otting, G.; Vasudevan, S. G.; Lescar, J.; Lim, S. P. A fluorescence quenching assay to discriminate between specific and nonspecific inhibitors of dengue virus protease. *Anal. Biochem.* **2009**, *395*, 195–204.

(31) Strelow, J.; Dewe, W.; Iversen, P. W.; Brooks, H. B.; Radding, J. A.; McGee, J.; Weidner, J. Mechanism of Action Assays for Enzymes. 2012; in G. S. Sittampalam et al. editors: Assay Guidance Manual. Bethesda (MD): Eli Lily & Company and the National Center for Advancing Translational Sciences; 2004-.

(32) de la Cruz, L., Nguyen, T. H. D., Ozawa, K., Shin, J., Graham, B., Huber, T., Otting, G. Binding of low molecular weight inhibitors promotes large conformational changes in the dengue virus NS2B-NS3 protease: Fold analysis by pseudocontact shifts. *J. Am. Chem. Soc.* **2011**, *133*, 19205–19215.

(33) Gibbs, A. C., Steele, R., Liu, G., Tounge, B. A., Montelione, G. T. Inhibitor bound dengue NS2B-NS3pro reveals multiple dynamic binding modes. *Biochemistry* **2018**, *57*, 1591−1602.

(34) Weigel, L. F., Nitsche, C., Graf, D., Bartenschlager, R., Klein, C. D. Phenylalanine and phenylglycine analogues as arginine mimetics in dengue protease inhibitors. *J. Med. Chem.* **2015**, *58*, 7719−7733.

(35) Bastos Lima, A., Behnam, M. A. M., El Sherif, Y., Nitsche, C., Vechi, S. M., Klein, C. D. Dual inhibitors of the dengue and West Nile virus NS2B–NS3 proteases: Synthesis, biological evaluation and docking studies of novel peptide-hybrids. *Bioorg. Med. Chem.* **2015**, *23*, 5748-5755.

(36) Noble, C. G.; Seh, C. C.; Chao, A. T.; Shi, P. Y. Ligand-bound structures of the dengue virus protease reveal the active conformation. *J. Virol.* **2012**, *86*, 438−446.

(37) Zapun, A.; Contreras-Martel, C.; Vernet, T. Penicillin-binding proteins and β-lactam resistance. *FEMS Microbiol. Rev.* **2008**, *32*, 361–385.

(38) Triboulet, S.; Dubée, V.; Lecoq, L.; Bougault, C.; Mainardi, J-L.; Rice, L. B.; Ethève-Quelquejeu, M.; Gutmann, L.; Marie, A.; Dubost, L.; Hugonnet, J-E.; Simorre, J-P.; Arthur, M. Kinetic features of L,D-transpeptidase inactivation critical for β-lactam antibacterial activity. *PloS One* **2013**, *8*, e67831.

(39) Edoo, Z.; Arthur M.; Hugonnet, J-E. Reversible inactivation of a peptidoglycan transpeptidase by a β-lactam antibiotic mediated by β-lactam-ring recyclization in the enzyme active site. *Sci. Rep.* **2017**, *7*, 9136.

(40) Wilmouth, R. C.; Westwood, N. J.; Anderson, K.; Brownlee, W.; Claridge, T. D. W.; Clifton, I. J.; Pritchard, G. J.; Aplin, R. T.; Schofield, C. J. Inhibition of elastase by *N*-sulfonylaryl β-lactams: Anatomy of a stable acyl-enzyme complex. *Biochemistry* **1998**, *37*, 17506–17513.

(41) van Soom, J.; Cuzzucoli Crucitti, G.; Gladysz, R.; van der Veken, P.; Di Santo, R.; Stuyver, I.; Buck, V.; Lambeir, A-M.; Magdolen, V.; Joossens, J.; Augustyns, K. The first potent diphenyl phosphonate KLK4 inhibitors with unexpected binding kinetics. *Med. Chem. Commun.* **2015**, *6*, 1954–1958.

(42) Moreno-Cinos, C.; Sassetti, E.; Salado, I. G.; Witt, G.; Benramdane, S.; Reinhardt, L.; Cruz, C. D.; Joossens, J.; Van der Veken, P.; Brötz-Oesterhelt, H.; Tammela, P.; Winterhalter, M.; Gribbon, P.; Windshügel, B.; Augustyns, K. α-Amino diphenyl phosphonates as novel inhibitors of Escherichia coli ClpP protease. *J. Med. Chem.* **2019**, *62*, 774–797.

(43) Nitsche, C.; Klein, C. D. Fluorimetric and HPLC-Based Dengue Virus Protease Assays Using a FRET Substrate. In Antiviral Methods and Protocols; Gong, E. Y., Ed.; Humana Press: New York, **2013**; Vol. 1030, pp 221–236.

(44) Trott, O.; Olson, A. J. AutoDock Vina: Improving the speed and accuracy of docking with a new scoring function, efficient optimization, and multithreading. *J. Comput. Chem.* **2010**, *31*, 455−1537.

(45) Morris, G. M.; Huey, R.; Lindstrom, W.; Sanner, M. F.; Belew, R. K.; Goodsell, D. S.; Olson, A. J. AutoDock4 and AutoDockTools4: Automated docking with selective receptor flexibility. *J. Comput. Chem.* **2009**, *30*, 2785–2791.

(46) Pettersen, E. F.; Goddard, T. D.; Huang, C. C.; Couch, G. S.; Greenblatt, D. M.; Meng, E. C.; Ferrin, T. E. UCSF Chimera-A visualization system for exploratory research and analysis. *J. Comput. Chem.* **2004**, *25*, 1605−1612.

(47) Metz, P., Chiramel, A., Chatel-Chaix, L., Alvisi, G., Bankhead, P., Mora-Rodriguez, R., Long, G., Hamacher-Brady, A., Brady, N. R., Bartenschlager, R. Dengue virus inhibition of autophagic flux and dependency of viral replication on proteasomal degradation of the autophagy receptor p62. *J. Virol.* **2015**, *89*, 8026–8041.

Table of Contents graphic